IN SITU CROSSLINKABLE POLYESTERS FOR TISSUE ENGINEERING AND DRUG DELIVERY

by

DIPENDRA RAJ GYAWALI

Presented to the Faculty of the Graduate School of
The University of Texas at Arlington in Partial Fulfillment
of the Requirements
for the Degree of

MASTER OF SCIENCE IN BIOMEDICAL ENGINEERING

THE UNIVERSITY OF TEXAS AT ARLINGTON
MAY 2009

ACKNOWLEDGEMENTS

I would like to thank Dr. Jian Yang for giving me such a wonderful opportunity to work in his laboratory and for being my advisor. Dr. Yang has taught me to seek answers and keep asking questions in the quest to become a better researcher. His constant motivation, guidance, and encouragement have helped me immensely in achieving all that I have during my years at UTA.

I would also like to thank Dr. Kytai Nguyen and Dr. Liping Tang for having spared their valuable time to review my work and also providing me with valuable suggestions whenever I have sought their help.

I would like to acknowledge Richard T. Tran for being with me throughout all the highs and lows of research. The countless hours spent in discussions and brainstorming with him has helped me to become more innovate and generate solutions to tricky problems that I faced in my research. I would like to extend my appreciation to my coworkers and friends Natasha KC, Parvathi Nair, Aleksey Kolasnikov, Yi Zhang, and Jagannath Dey for their continuous support and inspiration. I would also like to thank the lab members from Dr. Nguyen's lab and Dr. Tang's lab for allowing me to use their laboratory facilities.

It goes without saying that I owe everything to my family for their unstinting support, love, patience, and encouragement. They have given me every tool in life to seek and pursue all my goals.

April 16, 2009

ABSTRACT

IN SITU CROSSLINKABLE POLYESTERS FOR

TISSUE ENGINEERING AND

DRUG DELIVERY

Dipendra Raj Gyawali, M.S.

The University of Texas at Arlington, 2009

Supervising Professor: Jian Yang

In situ crosslinkable elastic materials are increasingly being explored for various biomedical applications such as drug delivery and tissue engineering due to their site specific nature. The creation of an *in situ* crosslinkable elastomer rich in pendant chemistry has been a challenge in the field of biomaterials. Herein, we have developed two new *in situ* biodegradable materials: poly(octamethylene maleate citrates) (POMC) and poly(poly(ethylene glycol) maleate citrate) (PPEGMC). These materials are all low molecular weight in their pre-polymeric form, which shows their potential to be used as an injectable biomaterial. The preservation of pendant carboxylic and hydroxyl groups in these polymeric networks after crosslinking were confirmed by structural and physicochemical studies. These networks are amorphous at body temperature with a T_g below 0 °C confirmed by DSC. Both materials are highly elastic and show no permanent deformation. The ultimate tensile strength and initial modulus are between 0.22 and 0.90 MPa, and 0.07 to 1.3 MP respectively. In vitro degradation studies confirmed the slower degradation rate of POMC when compared to that of PPEGMC (<60% total mass loss within 3

month period and >60% total mass loss with in 1 month period respectively). These properties can be tuned by varying the monomer molar ratio, initiator and crosslinker concentrations, and polymer concentrations while crosslinking. Photopolymerized POMC networks demonstrated good *in vitro* and *in vivo* biocompatibility. The drug and cell encapsulation ability of PPEGMC shows its potential use as an injectable material. These novel *in situ* hydrogel elastomers could have potential for the conjugation and encapsulation of biomolecules and for wound bandage/healing applications.

TABLE OF CONTENTS

LIST OF ILLUSTRATIONS

LIST OF TABLES

CHAPTER 1

IN SITU CROSSLINKABLE (ISC) POLYMERS

1.1 Introduction

Within the past few decades, the field of medical science has increased its demand for the development of novel biomaterials to solve unmet clinical needs. To meet the increasing demand, scientists have explored the versatility of polymer chemistry to meet specific requirements. In the course of development, in situ crosslinkable (ISC) polymers have gained serious attention (1). The use of this new class of polymers ranges from sample preparation for transmission electron microscopy (2) to scaffolding materials in the evolving field of tissue engineering (3), drug delivery (4), and wound managements. (5) In general, ISC polymers are materials that can be converted into a crosslinked network from a sol or moldable putties at the specified site (6). Solidification of these polymers is achieved *in situ* by various means such as free radical polymerization (7), thermogelling (8), ionic crosslinking (9) , self-assembly (10), and phase segregation (11). Free radical crosslinking, which has become a mainstay in the biomaterial arena, offers many advantages including superior mechanical properties and stability. More specifically, photoinitiated and redox-initiated free radical system are of great interest in the field of tissue engineering and drug delivery. In this system, free radicals are created in the initiation steps that further react with functional groups, often unsaturated bonds of the monomers or macromers, resulting in the propagation of crosslinking (12). Solidification mechanisms have a direct affect on the kinetics of the process and the stability of the resultant scaffolds. Therefore, it is equally important to understand the limitations of these crosslinking mechanisms. Table 1.1 summarized these different crosslinking mechanisms.

Table 1.1 Comparison between Redox-initiated and Photo-initiated free radical systems.

Redox-initiated	
Redox-initiated systems consist of a reducing and oxidizing agent that creates free radicals in an elevated temperature (13). Since this initiation does not utilize any external probe and can be crosslinked at physiological temperature, it has been recognized as an ideal initiating system to crosslink materials in vivo in orthopedic applications (14). Furthermore, due to the homogeneous crosslinking, it has been accepted for the fabrication of nanogels and microgels for drug delivery applications (15).	**Pros** ✓ This system can be used in areas of limited light penetration as is activated with temperature change (16). ✓ Initiators are homogeneously mixed with polymer solution that results in homogeneous crosslinking of the network (17). ✓ Various accelerators can be used to enhance the crosslinking time of the system (18). **Cons** X Crosslinking begins as soon as the initiating system is introduced thus can be an issue for prefabricating devices as entrapped air bubbles can adversely affect quality and mechanical performance. X Crosslinking cannot be stopped once it begins leading to poor temporal and spatial control over the system (12). X Elevated temperatures are often required for crosslinking, which may not be applicable for highly temperature sensitive biomolecules encapsulation (19).
Photo-initiated	
The concept of using photo-initiated systems to crosslink or polymerize materials in vivo has been wildly accepted and practiced in accessible place such as skin wound management, and the oral cavity in dentistry. Through a minimally invasive surgery, the hope is to prevent restenosis after angioplasty or postsurgical adhesions (20). Due to temporal and spatial control, photo polymerization is desirable for the fabrication of scaffolds for the engineering highly organized tissue such as vascular tissue and nerve regeneration. The choice and concentration of the photoinitiator, polymer, reactive double bonds, and light intensity can control rate of polymerization (21).	**Pros** ✓ Facilitate the processing of the system due to the control over the handling time and the initiation of the reaction (22). ✓ Offers temporal control of the initiation process. It may be beneficial for designing a system that needs a partial pre-implant and full post-implant crosslinking (23). ✓ Increase in temperature while crosslinking can be avoided with the concept of temporal control that prevents extensive narcosis of tissue at the implantation site (24). ✓ Offers spatial control over the system that is beneficial for development of complex structures such as patterned surfaces (12).

Table 1.1 – continued

.	✓ Crosslinking can be achieved under mild conditions such as room temperature, physiological temperature, and pH to allow for the incorporation of biologically active molecules and in vivo reactions without harm. (25) **Cons** X Ultraviolet rays can be an issue for some application such as cell encapsulation if exposure is not limited within few minutes (26). X Unsuitable for applications where light penetrated depth is limited. (16) X Cannot be carried out uniformly in a large or thick system due to inhomogeneous light distribution (16). X Colorization of the macromers can void the activation of initiator by absorbing the UV light (13).

It may be noted from Table 1.1 that redox-initiated and photo-initiated systems have their own limitations. In order to utilize them in the fabrication of ISC polymers, it is necessary that we first understand application of ISC in the field of tissue engineering and drug delivery.

1.2 ISC polymers in tissue engineering

The term “tissue engineering” was first recognized at a committee meeting of the National Science Foundation in early 1987 (27). Since then, a myriad of ideas have been developed to fulfill the primary goal of tissue engineering, which is to regenerate and restore the function of damaged tissues and organs (28). The general concept of tissue engineering is to direct cell proliferation and differentiation towards a targeted tissue by culturing a specific cell type in a microenvironment, which has been designed to mimic the native extra cellular matrix

(ECM) (29). However, imitating the process of nature according to our needs has been very difficult.

One strategy in tissue engineering is the use of polymeric scaffolds as a space filling material (30) or scaffolding for cell growth (31, 32). Unfortunately, pre-fabricated scaffolds are often used in this process where cell migration is the only method of infiltration (12). This limitation has led to the development and use of ISC polymers for cell encapsulation within biomaterials, which has shown potential in developing a construct with a homogeneous distribution of cells and uniform tissue growth (33). ISC materials offer many advantages over pre-fabricated scaffolds for certain applications (1). For example, ISC materials can be used as injectable scaffolds for tissue regeneration through a minimally invasive delivery method. In addition, injectable biomaterials may fill irregular defects by taking the shape of the cavity in which they are placed, thus avoiding the need for patient specific scaffold pre-fabrication (34). Similarly, the tissue-polymer adhesion and interaction is significantly improved during in vivo polymerization from the creation of surface microroughness (19). However, numerous requirements exist for scaffold design depending on the application, but certain material properties must be considered for all tissue engineering applications:

a. Biocompatibility: ISCs must be compatible with cells, tissues, and bodily fluids in order to function properly and avoid complications. As ISCs polymers can be used as an injectable or pre-fabricated scaffold, any leachable compounds and degradation products should not obstruct the process of tissue formation (35). Since ISCs are often used as scaffolds for carrying cells and sensitive compounds, the crosslinking process after injection should occur under physiologically accepted conditions (1).

b. Mechanical Properties: It is critical that the mechanical properties of the scaffold materials match with the tissues or organs being targeted (36). It has been recognized that the mechanical properties of scaffolds have an influence on the

inflammatory response, angiogenesis, and wound healing (37). Biomaterials implanted inside the body are subjected to a mechanically dynamic environment, and must be able to sustain and recover from repetitive deformations while allowing material/tissue integration without irritating surrounding tissues(38). ISC used for load bearing tissues should also possess sufficient mechanical strength for proper tissue regeneration (1). Most of the tissues in the body, however, are soft and highly elastic in nature (Table 1.2). To mimic these properties, the development of elastomeric materials is a new trend in the biomaterial society (38-41). The chemical structure, crosslinking mechanism, crosslinking density, and swelling ability are some of the important parameters that govern the overall performance of the scaffold.

Table 1.2 Mechanical properties of soft tissues.

Soft Tissues	Tensile Strength (Mpa)	Modulus (Mpa)	Elongation (%)	Ref.
Human bladder	0.27±0.14	0.25±0.18	0.69±0.17	(42)
Rat bladder	0.72±0.21	0.76±0.44	2.03±0.44	(42)
Pig bladder	0.32±0.10	0.26±0.18	1.66±0.31	(42)
Human myocardium	0.003-0.015	0.02-0.50		(43)
Porcine aortic heart valve (Radial)	1.40±0.20	6.40±0.90	134.80±27.70	(44)
Smooth muscle relaxed		0.006	300	(45)
Smooth muscle contracted		0.01	300	(45)
Carotid artery		0.09±0.02		(46)
Knee articular cartilage		2.10-11.80		(47)

c. Degradation: Biodegradation is a process by which polymers are chemically broken down into their precursor monomers, which can be accomplished through

dissolution, hydrolysis, and various enzymatic activities (48). Hydrolytic degradation is preferred over other methods because of minimal site-to-site and patient-to-patient variations (48). The presence of an ester functional group in the polymer main chain is a characteristic that distinguishes polyesters from classes of polymers (49). Due to their ease of degradation by hydrolysis, various families of polyesters have gained increased attention in tissue engineering (48). In addition to chemical structure, physical properties such as crystallinity, crystal structures, molecular orientation, melting temperature (T_m), glass transition temperature (T_g), crosslinking density, and external particulates present in the polymer network also influence the degradation rate (50).

d. Biofunctionalization: As mentioned above, synthetic materials are used to mimic the natural ECM. The ECM not only provides mechanical support but also regulates the cell's dynamic behavior including cells anchorage, segregation from one another, regulation of intercellular communication, and the direction of cell differentiation (51). To meet these versatile characteristics, the ECM is composed of various polysaccharides and fibrous proteins (52). In order to mimic the characteristics of the natural ECM, biomaterials should express sufficient functionality to conjugate with various biomolecules. A successful drug delivery vehicle can be constructed if the material expresses the proper functionality to conjugate with antibodies and ligands (53). Creating the necessary functional groups on the surface and in the bulk material remains a challenge for various thermally cured materials. Many approaches have been adopted to introduce functional groups on the surface of these polymers such as bulk chemical modification (54), surface hydrolysis (55), free radical grafting (56), and plasma treatment (57). Unfortunately, these techniques are only applicable for prefabricated scaffolds. Free radical crosslinking may offer great advantages for conserving available functionality such as amine, carboxylic, and

hydroxyl groups of the polymer that can be further utilized for surface or bulk conjugation of bioactive molecules to enhance cellular responses.

e. Porosity: A successful ISC scaffolds should possess highly porous and interconnected networks. These void spaces within the scaffold network support cellular in-growth and facilitate the exchange of nutrients and waste products (1). Although various methods such as gas foaming and particulate leaching have been established to generate porous scaffolds in situ, (33) the challenge still lies in the creation of an injectable scaffold with an interconnected and homogeneous pore network.

1.3 ISC polymers in Drug Delivery

In past few decades, a wide variety of drugs have been discovered and introduced for human use. Unfortunately, these drugs may create severe side effects to hinder their therapeutic efficacy. The concept of delivering drugs locally to a designated area has been recognized as an urgent focus to improve the efficacy and to reduce drug toxicity (58). In the course of developing advanced drug delivery systems, biomaterials have gained abundant attention. The drugs are encapsulated (59) or covalently bonded (60) with degradable bonds to the polymeric system with the hope of controlled release at the appropriate site. Similarly, if the delivery system can be functionalized with targeting biomolecules, a targeted drug delivery system can be designed (61). In order to be a good candidate for delivery system, biomaterials should possess specific physical, chemical, biological, biomechanical, and degradation properties.

While designing delivery system, serious consideration has to be made in three different stages:

a) Loading strategy: One of the primary considerations in drug delivery design deals with methods to load a specific drug or cell type in the polymeric matrix. Polymeric matrices herein can be macrogels, microgels, or nanogels according to the particular application (62). For pre-fabricated vehicles, the only way to load these drugs or cells is through

infiltration while soaked in the solution, which has been shown to have poor loading efficiency (63). Hence, ISCs can be a better option as it allows drugs or cells to be encapsulated while crosslinking. Furthermore, an injectable drug delivery system for site-specific applications can be designed through the use of ISCs (64).

b) Site-specific targeting: Targeted drug delivery represents one of the most active areas of advanced biomaterials. A typical targeted drug delivery system should consist of a polymeric system that can entrap therapeutics in the inner core and should be heavily functionalized on their outer surface to permit conjugation with targeting moieties (65). In addition, the circulation time of the delivery vehicles in the blood stream has also been shown to depend on the surface chemistry of the materials. For example, hydrophilic polymers such as poly(ethylene glycol) (66, 67) and N-(2-hydroxypropyl)methacryl- amide (68) were reported to have longer circulating times. Finally, the delivery vehicles should also provide a physical barrier to protect encapsulated therapeutics from degradation or premature metabolism during the delivery to the targeted site.

c) Release Profile: The ultimate goal of these delivery devices is to release intact therapeutics. Although zero order kinetics are the ideal release profile, most of the current system shows a rapid burst-type release followed by a slower controlled release (64). This initial burst of drug may irritate the surrounding tissue causing systemic toxicity. On the other hand, specific release profiles such as continuous release, pulsatile release, and release response to stimulus are some interesting aspects that solely depend on the chemical composition of the polymeric system (65).

1.4 Current ISC Polymers for Tissue engineering and Drug delivery

1.4.1 ISC Polyester Elastomers

Early this decade, the need of polyester elastomers in the field of tissue engineering and drug delivery was realized. This movement led to the development of numerous elastomers

including poly(glycerol sebacate) (PGS) (38), poly(diol citrate) (POC) (41) , poly(PEG-co-CA) (PEC) (39), poly(1,2-propanediol-sebacate)-citrate) (PPSC) (69), poly(1,8-octanediol malate) (POM) (40), and crosslinked-doped polyesters (CUPE) (70). These elastomers have promising characteristics for the engineering of tissues such as cartilage (71), myocardial tissue (72), vascular grafts (73), and annulus fibrosus regeneration (40). The basic characteristics of these elastomers include elasticity under cyclic stress, ease of hydrolysis, and tunable mechanical properties, and controlled degradation profiles. All these elastomers comprise of two distinct synthesis steps. First, linear pre-polymeric chains containing ester bonds and pendent groups were synthesized. Second, these linear chains were thermally crosslinked at elevated temperatures (>80 °C) and reduced pressure (<100 mTorr) for long periods of time (>24 h) to fabricate the desired scaffolding system.

It has been shown that these elastomers demonstrate excellent biocompatibility and are able to match the mechanical properties of various soft tissues. However, these materials are not capable of encapsulating temperature sensitive molecules and cells due to their harsh processing conditions. The acrylation of the pendent hydroxyl groups in the PGS pre-polymer was considered to develop a photocurable elastomer, poly (glycerol-*co*-sebacate) acrylate (PGSA) (74). It was reported that the properties of PGSA could be tuned according to the degree of acrylation to the pendent functionalities (74). PGSA was also reported as a porous cell-encapsulating matrix (75). As mentioned earlier, the ECM not only provides mechanical support but also provides chemical cues to enhance cellular responses. However, all the above-mentioned elastomers lack pendent functionality in bulk of the material for the biofunctionalization required for targeted applications of tissue engineering and drug delivery. Thus, the development of ISC elastomeric polyesters with adequate surface and bulk pendent functionality is important in the field of biomaterials.

1.4.2 ISC Hydrogels

Hydrogels are hydrophilic networks that swell under hydrated conditions (76). This class of polymer has been extensively utilized in variety of biomedical applications due to their high water content and rubbery nature comparable to natural tissues (77). These hydrogels can be synthesized from naturally derived extracellular matrix (ECM) precursors or synthetic precursors. The examples for the former are the hydrogels based on chemically modified glycosaminoglycans (GAGs) such as hyaluronan (HA) and chondroitin sulfate (CS) (78, 79). Hydrogels fabricated from cellular components are attractive because the ECM components may provide biological cues and guide or induce tissue-specific regeneration. However, these types of materials also bring concerns on their cost-effectiveness, potential immune responses, and batch-to-batch variations common to many other naturally derived materials used *in vivo*.

Synthetic crosslinkable hydrogels, such as poly (ethylene glycol), poly (vinyl alcohol)-,(80, 81) poly (propylene fumarate) (PPF)-,(82, 83) polyphosphoester-,(84, 85) and polylactone (such as PLA and PCL)(86, 87)-based hydrogels, have also attracted intense research focus recently. These hydrogels share a common ground in that vinyl groups are introduced into the base polymers to form crosslinkable precursors, which can be crosslinked *in situ* by photoinitiators or redox initiators. Most of these hydrogels were proposed for tissue engineering hard or stiff tissues such as bone or cartilage. For soft tissue applications, it is desirable that the properties of the biomaterials used should resemble those of the soft and elastic native ECM.

1.5 Objectives of this Research

POC has been recognized as an elastomer with excellent biocompatibility, hemocompatibility, tunable degradability, and mechanical properties comparable to natural soft tissues. However, the crosslinking strategy comprises of harsh conditions that void the encapsulation of temperature sensitive biomolecules and cells. In addition, the post-polymerization of POC scarifies all pendent functionalities once present in the pre-polymer. The rationale behind this study is to develop and characterize novel ISC polymers, poly (octamethylene maleate citrate)

(POMC) and poly (poly (ethylene glycol) maleate citrate) (PPEGMC) based on POC. By introducing maleate groups into the pre-POC backbones, POMC allows for free radical crosslinking to form a crosslinked network. The unreacted rich –COOH and –OH on the pre-POMC backbone can potentially be used as bioconjugation sites if proteins (such as collagen and antibodies), drugs, or peptides (such as RGD) are needed to confer biological functions to the materials. POMC should preserve the benefits of elastomeric POC including tunable mechanical properties, degradability, excellent biocompatibility, convenient synthesis, and cost-effectiveness. In addition to the previous benefits, *in situ* crosslinking capabilites are also present in this new generation of elastomers, and can be carried out using either photo or redox initiators in a rapid manner. The hydrophobic and short chain diol (1,8-octanediol) of POMC can be replaced with poly (ethylene glycol) of molecular weight 200 Da to create PPEGMC. This should increase the molecular weight between crosslinks and also avoid the use of organic solvents. These properties should make PPEGMC an injectable material for the delivery of cells and other therapeutic agents required in tissue engineering and drug delivery applications.

1.5.1 Specific Aims

a. Aim 1: To develop an *in situ* crosslinkable elastomer POMC with adequate pendent chemistry for the attachment of bioactive molecules.
b. Aim 2: Synthesize and characterize a new hydrogel PPEGMC for cell encapsulation and drug delivery system.

1.5.2 Successful Outcome of This Research Project

The successful outcome of this research project would provide a novel *in situ* crosslinkable biodegradable biomaterial that can be used as a functionally rich elastomer or an injectable hydrogel. It is expected that this study will help to understand this new polymeric network in designing an injectable materials for tissue engineering and drug delivery applications.

CHAPTER 2

POLY(OCTAMETHYLENE MALEATE CITRATES)(POMC)

2.1 Introduction

The previously developed biodegradable elastomeric polymer, poly(1,8-octanediol citrate) (POC) holds a promising future in the field of tissue engineering. Owing to its good biocompatibility, elastomeric properties, and inherent biodegradability, this polyester elastomer is suitable for soft tissue applications. However, it fails to serve as an injectable scaffolding material due to its processability. In the process of post polymerization, POC not only goes through harsh conditions (>80° C, <5pa and >24 h), but also scarifies all the pendent functionality once present in its pre-polymeric form.

Herein, a new *in situ* crosslinkable biodegradable elastomeric biomaterial, poly (octamethylene meleate citrates) (POMC) is reported. This new class of synthetic, elastomeric, and biodegradable polyester is composed of 1,8-octanediol (OD), maleic acid (MA), and citric acid (CA). Maleic acid was chosen as a difunctional acid containing vinyl functionality. When in its saturated ester form, it is known as succinate (88), which is an important component of the citric acid cycle and has been used in many synthetic biomaterial designs (89-91). Citric acid is a multifunctional acid that is a metabolic product of the Krebs cycle (92). 1,8-octanediol is a water-soluble diol with demonstrated biocompatibility. In the present work, structural analysis, thermal and mechanical properties, swelling, sol-gel fraction, surface modification, biocompatibility, *in vitro* degradation, and the processability of the POMC have been thoroughly investigated. The preliminary exploration of using the *in situ* crosslinkable POMC as a liquid wound dressing/bandage material is also reported.

2.2 Materials and Methods

2.2.1 Materials

All chemicals, cell culture medium and supplements were purchased from Sigma-Aldrich (St. Louis, MO), except where mentioned otherwise. All chemicals were used as received.

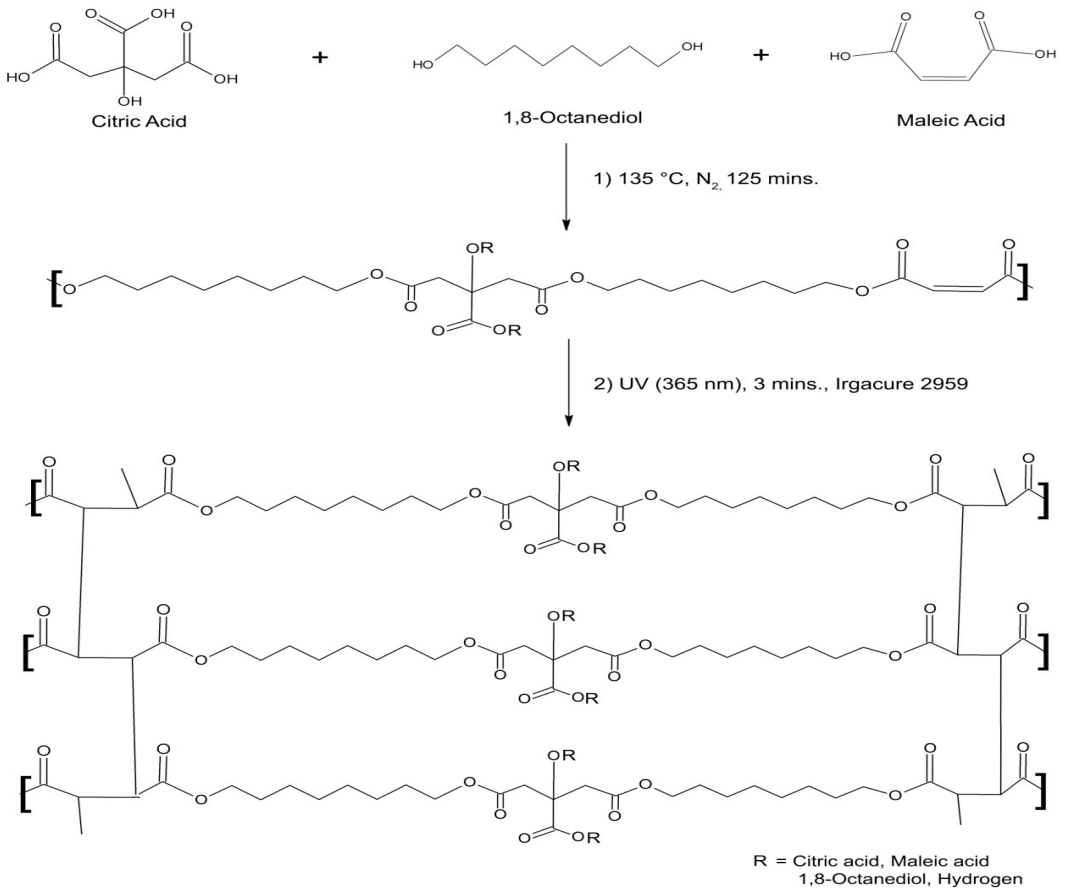

Figure 2.1 Synthesis Scheme of POMC. The synthetic scheme comprise following steps: 1) Synthesis of pre-POMC incorporating the following monomers: a multifunctional (carboxylic acid) Citric Acid, Vinyl functional Maleic Acid, Alcohol containing 1,8-octanediol. Ratios of Maleic Acid and Citric Acid were varied as 10/0, 8/2, 6/4, 4/6, and 2/8 respectively, where as ratio of overall acid to alcohol was kept as 1:1. All the monomers were melted at 160 °C under nitrogen blanket. Further polymerization was continued at 135 °C for 125 minutes to achieve low molecular weight pre-polymer. Photocrosslinking of polymer was performed under 365 nm ultraviolet light for 3 minutes in presence of photoinitiator (Igacure2959).

2.2.2 Synthesis of Pre-POMC

All the chemicals were purchased from Sigma-Aldrich (Milwaukee, WI) and used as received. The synthesis of POMC was carried out as shown in the schematic in Figure 1. CA, OD, and MA were added into a 250 mL three-necked round bottom flask fitted with an inlet adapter and outlet adapter. The mixture was melted within 20 minutes by stirring the contents in the flask at a temperature of 160 °C under nitrogen gas flow. Once the constituents melted, the temperature was reduced to 135 °C and the reaction was allowed to progress for an additional 125 minutes under a nitrogen purge to create the pre-POMC. Pre-POMC was dissolved in 1, 4-dioxane, and precipitated in de-ionized water in order to remove any un-reacted monomers. The precipitated polymer solution was freeze-dried to obtain the purified pre-POMC. To investigate the effects of the reactant ratio on the properties of the polymer, five different molar ratios of maleic acid to citric acid were studied (10/0, 8/2, 6/4, 4/6 and 2/8) respectively as shown in Table 2.1. The ratio of the acids over the diol for the reaction was kept as 1:1.

Table 2.1 Feeding ratio and actual composition of pre-POMC**.**

Polymer Name	MA:CA:OD (moles)	Feeding Ratio MA:CA:OD	Composition MA:CA:OD
POMC (10/0)	0.10/0.00/0.10	0.5/0.0/0.50	0.51/0.0/0.49
POMC (8/2)	0.08/0.02/0.10	0.4/0.1/0.50	0.38/0.12/0.51
POMC (6/4)	0.06/0.04/0.10	0.3/0.2/0.50	0.29/0.21/0.49
POMC (4/6)	0.04/0.06/0.10	0.2/0.3/0.50	0.19/0.32/0.49

2.2.3 Characterization of Pre-POMC

The average molecular weight of the pre-POMCs were analyzed by an Autoflex Matrix Assisted Laser Desorption/Ionization Mass Spectroscopy (MALDI-MS) (Bruker Daltonics, Manning Park, MA). 2-(4-hydroxyphenyl-azo)-benzoicacid (HABA) was used as the matrix to

mix with the pre-POMCs in a 1:1000 pre-polymer:matrix molar ratio. The functional groups present in the pre-polymers were analyzed by Fourier Transform Infra Red (FT-IR) spectroscopy using a Nicolet 6700 FT-IR (Thermo Scientific, Waltham, MA). Pre-POMCs were dissolved in dimethyl sulfoxide-d_6 (DMSO-d_6) in a 5-mm-outside diameter tube and analyzed by Proton Nuclear Magnetic Resonance spectroscopy (^{1}H NMR) using a 250 MHz JNM ECS 300 (JEOL, Tokyo, Japan). The chemical shifts for the ^{1}H NMR spectra were recorded in parts per million (ppm), and were referenced relative to tetramethylsilane (TMS, 0.00 ppm) as the internal reference.

2.2.4 Preparation and Characterization of Photocrosslinked POMC

Pre-POMC was crosslinked by free radical polymerization. The purified pre-polymer was dissolved in dimethylsulfoxide (DMSO) to make a 50% polymer by weight concentration. To generate the free radicals, 2% (w/w) of the photoinitiator (PI) 2-hydroxy-1-[4(hydroxyethoxy)phenyl]-2-methyl-1 propanone (Irgacure 2959) was dissolved in the polymer solvent solution. Next, the solution was poured into a Teflon mold and placed under a UVP 365 nm Long Wave Ultraviolet Lamp (Upland, CA) for 3 minutes. The thermoset elastomer achieved through this process is shown in Figure 1. The crosslinked polymer was placed in an excess amount of DMSO for twenty-four hours to remove any unreacted polymer, and then exchanged with water for another twenty-four hours. Finally, the purified crosslinked polymer was achieved by freeze-drying for 3 days. Photocrosslinking of POMC2/8 with the desired amount of PI (<5%) was not achieved, so it was not considered for further characterization. Bond vibrations of crosslinked film of POMC were evaluated using FTIR spectroscopic analysis.

2.2.5 Thermal Characterization of Photocrosslinked POMC

The thermal behaviors of the crosslinked films of three different ratios of POMC were studied on a DSC550 (Instrument Specialists Inc., Spring Grove, IL) and TGA (Thermogravimetric Analysis, Mettler Toledo, Columbus, OH). For the DSC analysis, samples were first scanned up to 150 °C at a heating rate of 10 °C/min under nitrogen purge (50 ml/min) to remove any traces of water from the sample. Thereafter, the samples were rapidly cooled at

a cooling rate of -40 °C/min to -60 °C. The samples were scanned again for the second time up to 230 °C at a heating rate of 10 °C/min. The glass transition temperature (T_g) was determined as the middle of the recorded step change in heat capacity from the second heating run. Similarly, TGA thermograms were observed under the flow of nitrogen gas (50 ml/min) at a scanning speed of 101 °C/min in the range of 50–600 °C. The decomposition temperature (T_d) was defined as the temperature at which 10% weight loss of the samples occurred.

2.2.6 Mechanical Properties of Photocrosslinked POMC

The tensile mechanical properties were studied according to the ASTM D412a standard on an MTS Insight II mechanical tester equipped with a 500 N load cell (MTS, Eden Prairie, MN). Crosslinked POMC films were cut using a dog bone shaped (26 mm × 4 mm × 1.5 mm; length × width × thickness) aluminum die. The dog bone shaped films were pulled until failure at a rate of 500 mm/min to obtain the stress strain curves. The initial slope (0-10%) of the curve was used to determine the modulus of the material. A detailed study on the effect of different ratios of the monomers, the amount of PI, and concentration of the polymer in solvent on mechanical properties of the polymer was performed. The density was measured using a Mettler Toledo balance equipped with a density determination kit (Greifensee, Switzerland) based on Archimedes' principle.

2.2.7 Swelling Ratio Measurements

Purified POMC was fabricated according to the process mentioned above. Six polymer discs (7 mm in diameter) were cut from the crosslinked films using a cork borer. DMSO was used as the swelling agent in this study due to its high boiling point, and deionized water was used to observe the water uptake of the polymer. Swelling studies were also conducted in PBS (pH 7.4 at 37 °C). The discs were allowed to swell in the respective swelling agents until the equilibrium state was achieved (2 days). The surface of the swollen discs was gently blotted with filter paper to remove any excess swelling agent, and the sample was then weighed (M_w). The discs were freeze-dried for 3 days and weighed to determine the dry weight (M_d). The equilibrium swelling ratio was calculated by Equation 1. The experiment was repeated three

times and the average value was reported. The effects of polymer concentration and PI concentration on sol-gel fraction were also evaluated in this experiment.

$$\%SR = \frac{(M_w - M_d)}{M_d} \times 100 \qquad (1)$$

2.2.8 Sol Gel Fraction Measurements

Six polymer discs (7 mm in diameter) were cut from the crosslinked films using a cork borer. The discs were weighed to find the initial mass (M_i), and suspended in DMSO for twenty-four hours. The DMSO was changed every six hours. Next, the discs were placed in water to exchange DMSO for twenty-four hours and freeze-dried for seventy-two hours. The dried samples, absent of non crosslinked pre-polymer, were weighed to obtain (M_d). The sol gel fraction (SFG %) was calculated by Equation 2.

$$\%SGF = \frac{M_i - M_d}{M_i} \times 100 \qquad (2)$$

2.2.9 In Vitro Degradation Study

Six polymer discs (7 mm in diameter) were cut from the crosslinked films using a cork borer. The discs were weighed to find the initial mass (M_i), and suspended in PBS (pH 7.4) and maintained at 37 °C. The pH was monitored and the buffer was replaced every day for first week and every subsequent week to ensure a constant pH of 7.4. At the desired time point, the samples were rinsed with deionized water, freeze-dried, and weighed to find the remaining mass (M_t). The percent mass loss (%ML) was calculated by Equation 3.

$$\%ML = \frac{M_i - M_t}{M_i} \times 100 \qquad (3)$$

2.2.10 Collagen immobilization

POMC6/4 films (7 mm diameter; 2 mm thick) were washed by refluxing in anhydrous ethanol for 3 h and dried under vacuum. Next, the films were immersed into 10 mL of a 5 mM 2-(N-morpholino)ethanesulfonic (MES) buffer solution (pH 4.5). Carboxylic acids groups were subsequently activated with 9.3 mg EDC and 3 mg NHS for 2 h with mild magnetic stirring at 4

ºC. Additionally, 1.5 mL of a 10 mg/mL collagen hydrochloride solution was prepared in 20 mL of a 5 mM MES solution. The activated carboxylic acid group containing films were washed twice with the 5 mM MES solution, merged into the collagen solution, and gently agitated for 6 h at 4 ºC. Finally, the films were taken out, washed twice with deionized water, and dried by lyophilization.

2.2.11 In Vitro Cell Attachment and Proliferation

POMC6/4 was used a representative polymer for all cytotoxicity evaluation studies. Photocrosslinked and collagen immobilized POMC films were cut into discs (7 mm diameter; 2 mm thick) and sterilized in ethanol for 30 minutes, and placed under UV light for another 30 minutes. The disks were seeded with a seeding density of $3x10^5$ cells/mL (NIH-3T3 Fibroblasts and human aortic smooth muscle cells (HASMC)). The cells were allowed to proliferate in Dulbecco's modified eagle's medium (DMEM) with 10% fetal bovine serum (FBS) for 3 days in an incubator maintained at 37°C, 5% CO_2, and 95% humidity. The cells were then fixed in gluteraldehyde-PBS solution, stained with hematoxylin and eosin (H&E), and observed under an inverted microscope (Zeiss Auxiovert).

A methylthiazoletetrazolium (MTT) cell proliferation and viability assay was used for a quantitative assessment of the cell growth and proliferation on POMC films and collagen immobilized POMC films. Un-modified PLLA films were used as a control. Six discs (7 mm) of each film were cut and placed into 96 well plates. HASMCs were seeded on each of the film according to the seeding protocol mentioned above. MTT Assay analysis was performed for three time points (2, 5, and 7 days) as per the manufacturer's protocol. An Infinite200 microplate reader (Tecan Group Ltd., Switzerland) was used at 570 nm with a reference wavelength of 690 nm for absorbance analysis.

2.2.12 In Vivo Host Response

POMC8/2 discs (7 mm diameter; 2 mm thick), representative POMCs, were implanted in 7-week-old female Sprague-Dawley rats by blunt dissection under deep isoflurane-O_2 general anesthesia. Animals were cared for in compliance with the regulations of the Animal Care and

Use Committee of The University of Texas at Arlington. POMC samples were implanted symmetrically on the upper and lower back of the same animal. The rats were sacrificed and tissue samples surrounding the implants were harvested with an intact implant at 1 week and 4 weeks. Samples and surrounding tissue were frozen in OCT embedding media (Polysciences Inc., Warrington, PA) at -80 °C, sectioned and stained with hematoxylin & eosin (H&E) for histological evaluation. Images were taken at 10× magnifications using a Leica DMLP microscope fitted with a Nikon E500 camera (Nikon Corp. Japan). The line tool in the ImageJ Analysis Software was used to measure the thickness of the fibrous capsule. Readings from 10 different portions of each image were collected, and the averaged value was reported.

2.2.13 POMC Scaffold Fabrication

Scaffold sheets were fabricated using 5 x 5 cm Teflon molds. POMC8/2 pre-polymer and PI was dissolved in 1, 4-dioxane to form a 30% solution. Sieved salt (150-250 μm) was added in a 1:9 pre-polymer:salt weight ratio to form a thick slurry, which was cast into the Teflon mold. After solvent evaporation, the mold was placed under a UV lamp, and then transferred into an oven maintained at 80 °C for a period of 24 hours. The salt was removed by leaching in de-ionized water for a period of 72 hours with water changed every 6 hours. The scaffolds obtained after leaching were freeze-dried for 48 hours to remove all traces of water. The scaffold was then freeze fractured using liquid nitrogen, and the cross section of the fractured sample was examined under a Hitachi S-3000N scanning electron microscope (Hitachi, Pleasanton, CA).

2.2.14 POMC Nanoparticle Fabrication

A 5% (w/v) solution of POMC8/2 pre-polymer in acetone was prepared. The polymer solution was then added dropwise into stirred DI water. The mixture was allowed to stir at 1200 rpm for 6 hours to let the solvent evaporate. Dynamic Light scattering (DLS) test was used to measure the size and size distribution of the obtained nanoparticles. Transmission electron microscope (TEM 2 JEOL 1200EX II) was also used to observe the morphology of the nanoparticles.

2.2.15 In Situ Crosslinking of POMC as Wound Dressing

To demonstrate the *in situ* wound dressing rapid formation using POMC, several random contour geometries were made on porcine skin (Walmart, Arlington, Texas) using a razor blade. Pre-POMC8/2 was mixed thoroughly with 2% (w/w) of PI until a homogeneous paste was achieved. The paste was carefully smeared onto the various contour and placed under UV light for 3 minutes.

2.2.16 Statistical Methods

All the experiments were repeated three times and the average value was reported. Data are expressed as mean ± standard deviation. Statistical analysis was performed using one way-ANOVA with post hoc Neuman–Keuls testing to ensure that groups are statistically different. The swelling data and mechanical properties of the polymer were compared with one way ANOVA. Data were taken to be significant, when a p-value of 0.05 or less was obtained.

2.3 Results

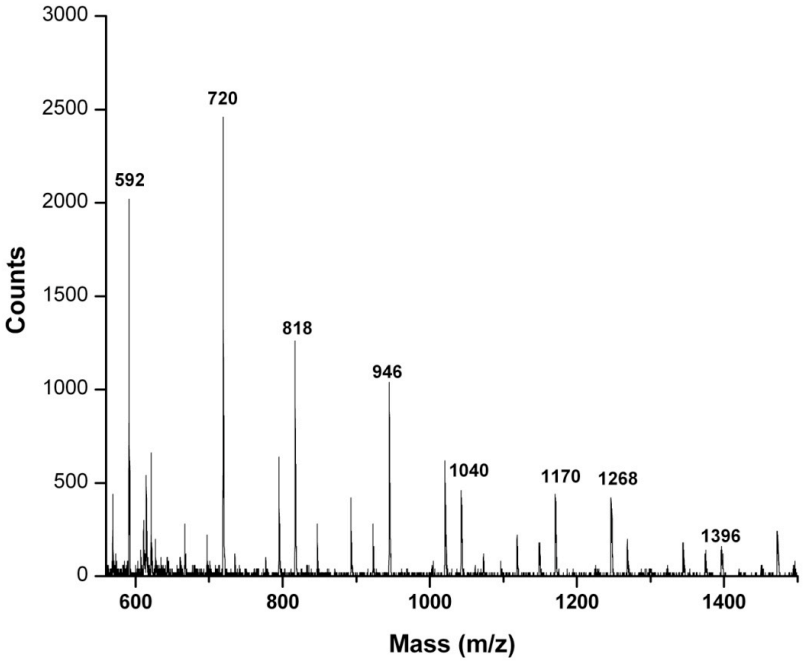

Figure 2.2 A typical MALDI-MS spectra of pre-POMC 8/2.

2.3.1 Characterization of pre-POMC

The average molecular weight of pre-POMC was measured by MALD-MS, and a typical spectrum of pre-POMC8/2 can be seen in Figure 2.2. The peaks from the main distribution and all the sub-distributions were taken in consideration in the calculation of average molecular weight of the pre-polymer. These spectra confirmed that a low molecular weight pre-polymer was synthesized with average molecular weight in the range of 701.23 to 1291.34 Da (Table 2.2).

Table 2.2 Mechanical properties of photocrosslinked POMC polymer films. Values are reported as the mean with standard deviation (n=6).

Samples	density	Initial Modulus	Tensile strength	Elongation	Average Mol. Wt.
	(g/cm^3)	(MPa)	(MPa)	(%)	Da
POMC (10/0)	1.124±0.002	0.48± 0.07	0.292± 0.075	55.02± 9.62	1291.34
POMC (8/2)	1.119±0.002	1.058± 0.11	0.88± 0.130	72.63± 7.74	874.59
POMC (6/4)	1.09±002	0.278± 0.05	0.55± 0.062	169.49± 36.57	769.34
POMC (4/6)	1.078±0.004	0.075±0.010	0.37± 0.067	322.09± 57.95	701.23

A typical ^{1}H NMR spectrum of POMC8/2 could be seen in Figure 2.3. The peaks (d) located at 1.53 ppm were assigned to in –O-$CH_2C\underline{H_2}$– from 1,8-octanediol. The peaks (b) located at 2.79 ppm were assigned to –$C\underline{H_2}$– from citric acid. The peaks located between 6 and 7 ppm were assigned to the protons of –C<u>H</u>=C<u>H</u>– incorporated into the polymer chain. The actual compositions of the pre-polymers were calculated based on the integration of the area under the characteristic proton peaks from each monomer: diol (d/4), CA (b/4), and MA (a/2). The actual polymer composition can be well controlled by varying the feeding ratio of the monomers as shown in Table 1.

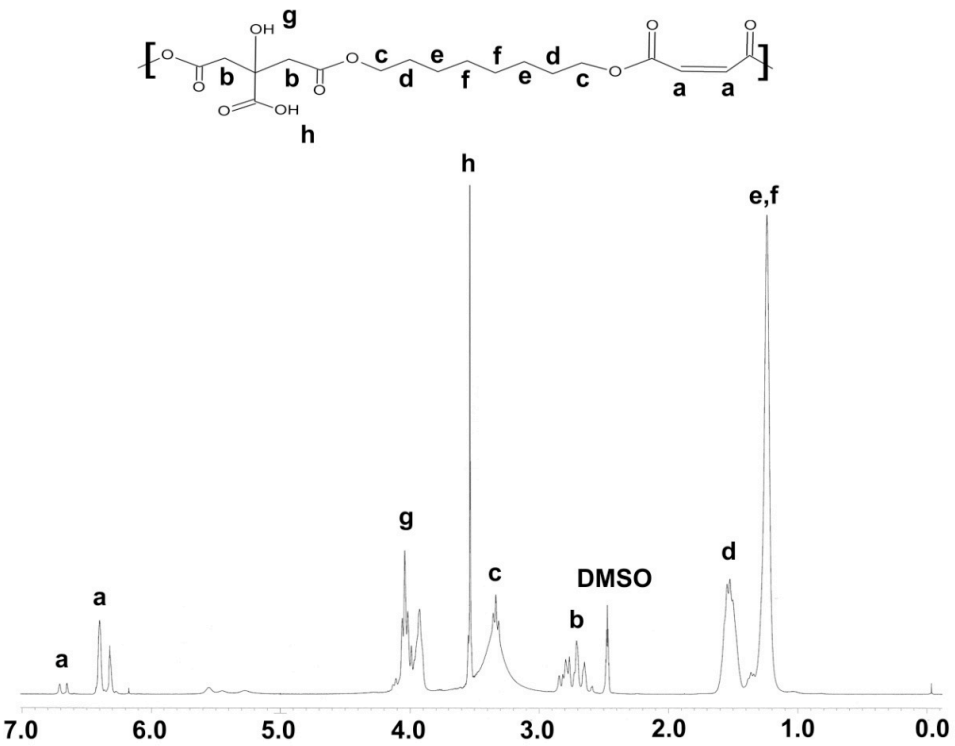

Figure 2.3 H^1 NMR spectra of pre-POMC8/2.

2.3.2 Characterization of Photocrosslinked POMC

Purified pre-POMC and POMC films were characterized by FT-IR as shown in Figure 2.4. The pronounced peaks within 1690–1750 cm^{-1} suggest the presence of carbonyl (C=O) groups from the ester bond and pendent carboxylic acid from the citric acid. The shoulder peak of a lower wavelength at 1650 cm^{-1} proves the presence of the olefin moiety from maleic acid. Similarly, the peak centered at 2931 cm^{-1} is evidence of the methylene groups from 1, 8-octanediol. Hydrogen bonded hydroxyl functional groups showed absorbance as a broad peak centered at 3570 cm^{-1} on both the prepolymer spectra and photocrosslinked film spectra. A shoulder peak at 1647 cm^{-1} due to C=C stretching exhibits higher absorbance in pre-POMC6/4 as compared to the POMC6/4 photopolymerized film, which indicates the reduction of the olefin moiety in the free radical polymerization crosslinking process. Similarly, the peak located at 869 cm^{-1}, which was found only in the pre-POMC, denotes the out-of-plane C–H bending of the conjugated olefin moieties.

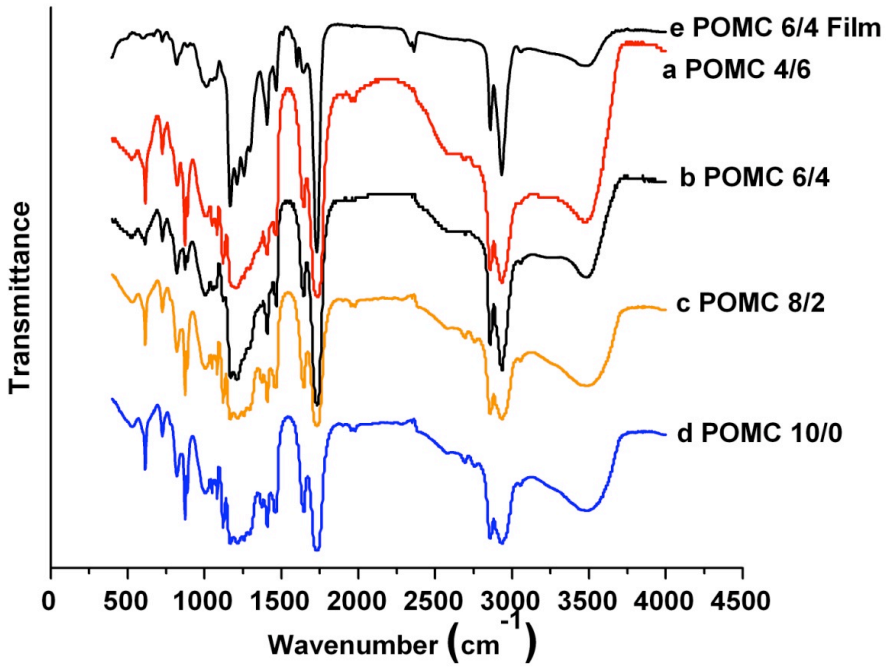

Figure 2.4 FTIR spectra of pre-polymers a. pre-POMC4/6, b. pre-POMC6/4, c. pre-POMC8/2, d. pre-POMC10/0 and POMC6/4 photocrosslinked film.

2.3.3 Thermal Characterization of Photocrosslinked POMC

The thermal stability of POMC was analyzed by TGA. Figure 2.5 graphically depicts the decomposition of the polymer as the temperature was increased. POMC4/6 exhibits 10% decomposition at 363.6 °C, whereas POMC10/0 displayed a 10% decomposition at 310.74 °C. These results confirm that as the amount of maleic acid is decreased, the polymer gains more thermal stability. The glass transition temperature (T_g) of the POMC films were analyzed with the aid of DSC. No crystallization or melting temperatures were observed in the thermograph.

As seen in Figure 2.6, the T_g of all the pre-polymers were below 0 °C, which indicated that all the polymers are amorphous at body temperature. The T_g of POMC4/6 was as high as -9.10 °C. POMC10/0 had the lowest T_g (-36.37 °C). Thus, the results from the Figure 3A show that as the amount of maleic acid was increased, the T_g of the polymer was decreased.

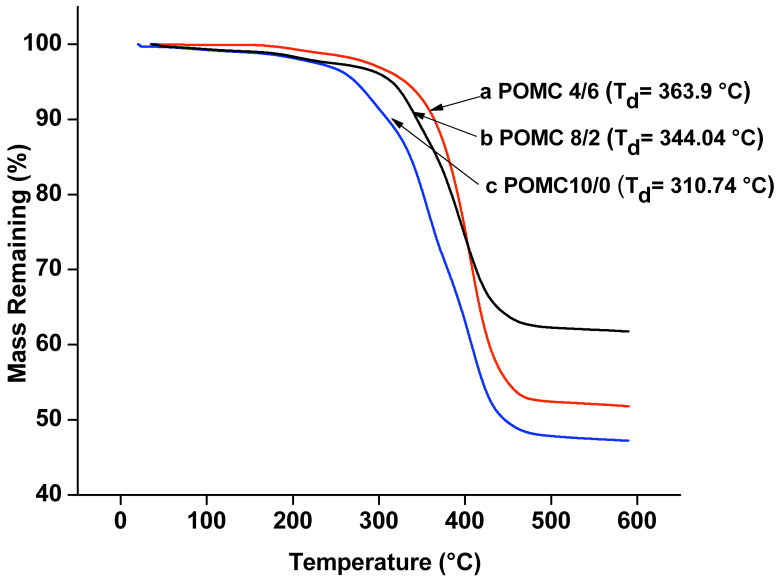

Figure 2.5 TGA graph of a.POMC4/6, b. POMC8/2, and c. POMC10/0 films decompose 10% of its total mass at 363.9 °C, 310.74 °C and 344.04 °C respectively.

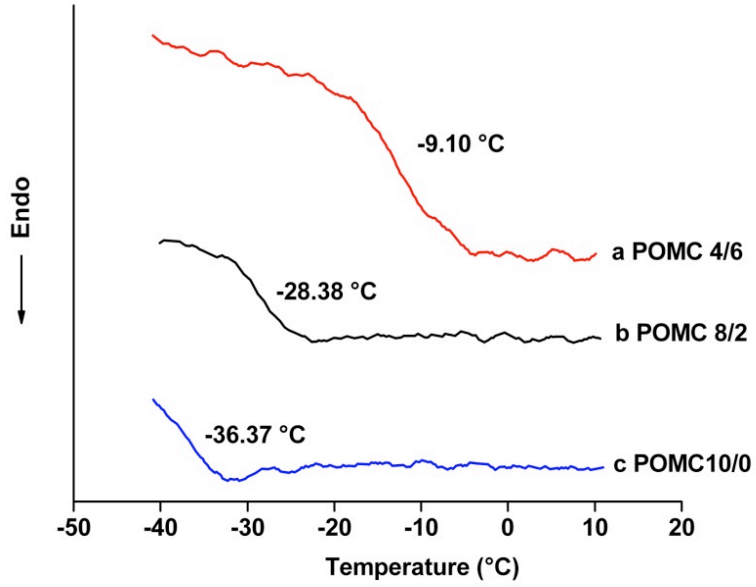

Figure 2.6 DSC thermograph of a. POMC4/6, b. POMC8/2, and c. POMC10/0 films with respective T_g at -9.10° C, -28.38° C, and -36.37°.

2.3.4 Mechanical Properties of Photocrosslinked POMC

Tensile mechanical tests on POMC samples showed that as the amount of maleic acid decreased, the elastomers became softer, and more elastic (Table 2.2). However, when no citric acid was used in the synthesis, a lower value for initial modulus (0.48±0.07 MPa) was found when compared to POMC8/2 (1.058±0.11 MPa). The effects of the PI and polymer concentration were also investigated. As the PI concentration increased from 0.25% to 1.0%, an increase in the initial modulus (0.075±0.004 to 1.058±.11 MPa) and decrease in elongation (276.87±11.7% to 62.63±19.8%) was seen (Figure 2.7A, $p<0.001$). However, the PI concentration had no further effect on the initial modulus and elongation after 1.0%. Similarly, the pre-polymer concentration also affected the mechanical properties of the crosslinked material (Figure 2.7B). It was observed that increasing the concentration of polymer while crosslinking from 30% to 100% resulted in a 6 fold increase in the initial modulus (0.207±0.042 MPa to 1.258± 0.115 MPa), and a 5 fold decrease in the elongation (199.66±40% to 40.38±2.34%). POMC8/2 crosslinked with 1% of PI and 50% polymer concentration was synthesized and hydrated for mechanical tests. There was no significant difference found in the initial modulus and elongation (figure 2.7C) Furthermore, the effects of the UV crosslinking time (3 to 30 minutes) were also studied, but no significant change in ultimate strain and stress was observed (data not shown). The densities of the POMC films were calculated according to Archimedes principle. It was observed that density decreased as the molar ratio of maleic acid decreased as seen in Table 2.2.

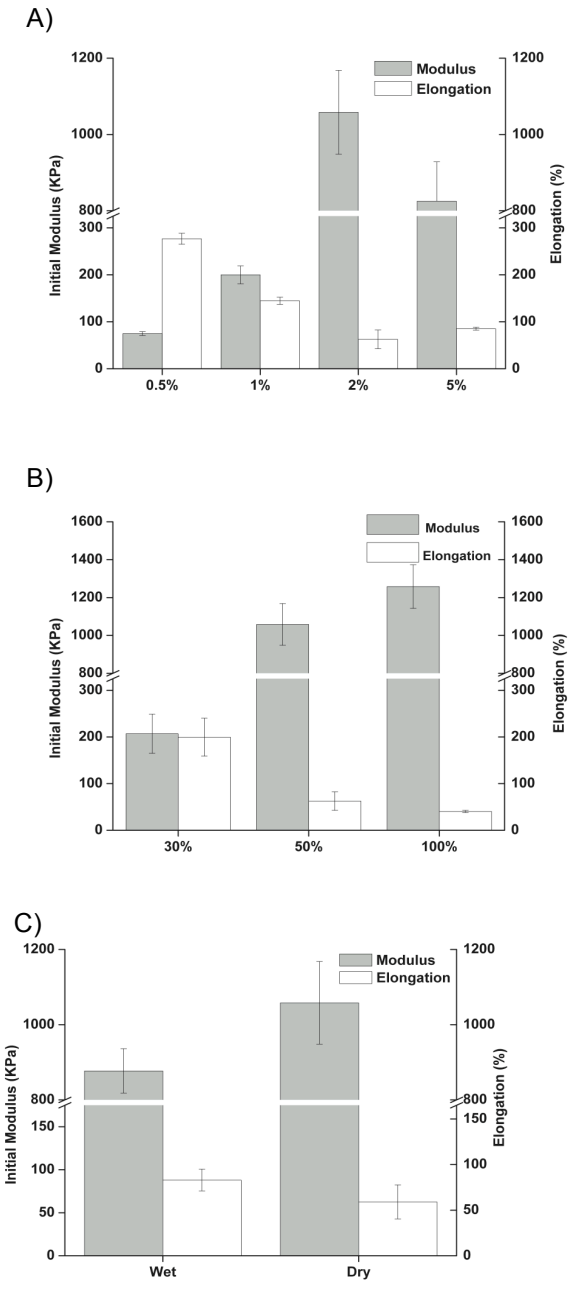

Figure 2.7 Mechanical Properties of photocrosslinked POMC with various polymerization conditions: A) effect of concentration of photoinitiator while crosslinking POMC8/2 with 50% polymer concentration in DMSO on Initial Modulus and Elongation of the film, B) effect of polymer concentration in DMSO while crosslinking POMC8/2 with 2% of photoinitiator concentration on Initial Modulus and Elongation of the film, C)wet and dry mechanical properties of POMC8/2 crosslinked with 2% of photoinitiator and 50% polymer on DMSO (n=6).

2.3.5 Swelling Properties and Sol Gel Fraction

In order to understand the swelling behavior of the polymer, detailed studies on the effect of monomer composition, PI concentration, and pre-polymer concentration were investigated. As seen in Figure 2.8A, as the amount of maleic acid was increased, the swelling capacity of the polymer decreased in all type of swelling agents (DMSO, PBS, and water). Similarly, a significant difference in the swelling behavior was observed when the PI concentration changed (Figure 2.8B, $p<0.05$). For example, the POMC films crosslinked by 0.25% PI had a swelling ratio of 9.03%, while the POMC films crosslinked by 1.0% PI concentration had a swelling ratio of 5.64% in DMSO. A significant difference was noticed on the swelling behavior when the concentration of polymer was varied (Figure 2.8C, $p<0.05$). The water uptaking ability of the polymer did not show any significant difference when changing the PI concentration. However, the polymer uptakes only 3.25±0.51% when crosslinked without any solvent and 25.18±5.22% when crosslinked with 70% of solvent in water.

The sol gel fraction of the crosslinked polymer was determined by soaking freshly crosslinked polymer discs in DMSO for two days. As seen in Figure 2.8A, as the molar ratio of maleic acid increased and polymer concentration decreased, there is significance decrease in sol fraction of the polymer ($p<0.05$). However, no significant difference in the sol gel fraction is seen when the amount of the PI concentration is varied (Figure 2.8B, 2.8.C).

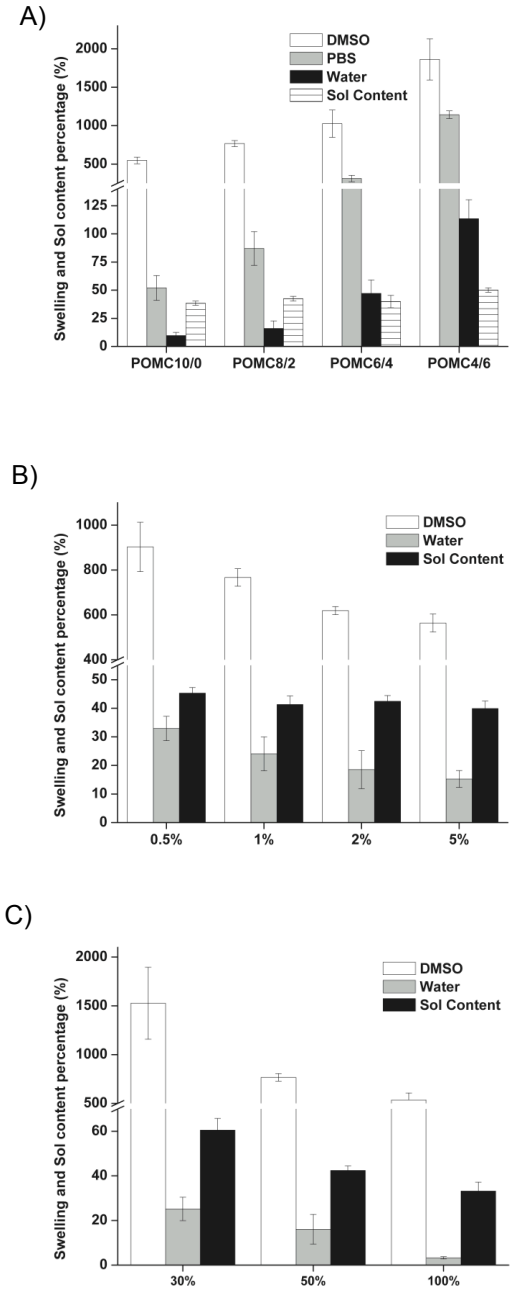

Figure 2.8 Swelling and sol content of photocrosslinked POMC with various polymerization conditions: A) effect of maleic acid and citric acid ratio crosslinked with 2% of photoinitiator concentration and 50% polymer concentration in DMSO, B) effect of concentration of photoinitiator while crosslinking POMC8/2 with 50% polymer concentration in DMSO, and C) effect of polymer concentration in DMSO while crosslinking POMC8/2 with 2% of photoinitiator concentration. Swelling agents herein are used as DMSO, PBS, and water. Sol content was leached out from the film in DMSO (n=6).

2.3.6 *Degradation of POMC*

Figure 2.9 shows the hydrolytic degradation rate of POMC polymer films with different monomer ratios in PBS at 37 °C. As the molar ratio of maleic acid is increased, the degradation rate is decreased. 70% of the polymer mass was lost within a three month time period for POMC4/6, where as only a 10% mass loss was observed on the POMC10/0 film.

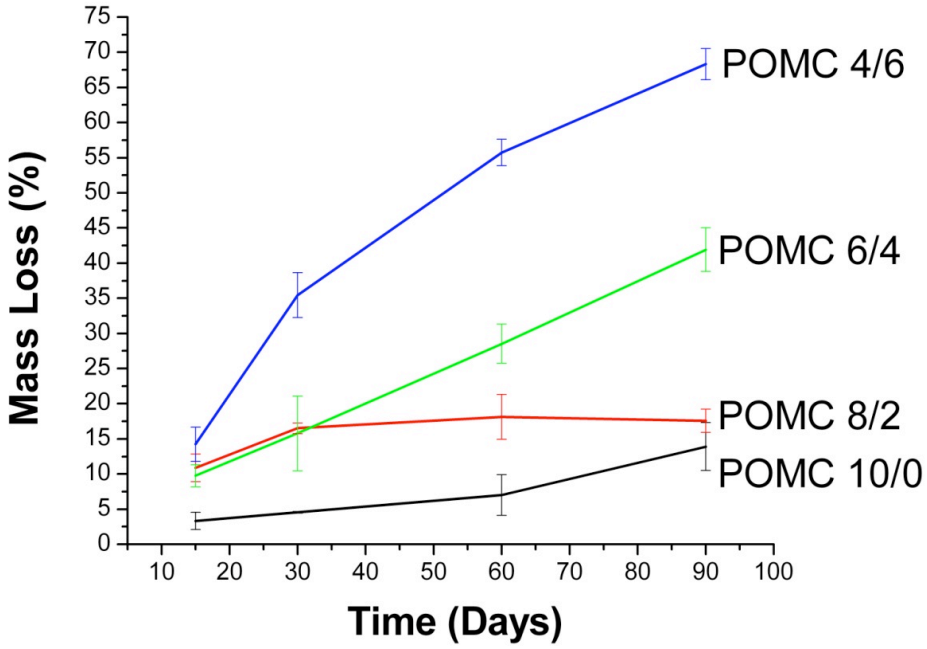

Figure 2.9 The effects of different POMC monomer ratios on the degradation rate in PBS (pH 7.4) at 37 °C. $p<0.05$. (n=6).

2.3.7 *Collagen Immobilization onto POMC*

When comparing the bond vibration peaks of POMC 6/4 and collagen immobilized POMC8/2 films, the appearance of a peak at 1648, 1544, and 3450 cm^{-1} correlate to amide I, amide II, and amine groups respectively. Figure 2.10 shows the successful introduction of amide groups to the polymer surface achieved from the immobilization of collagen.

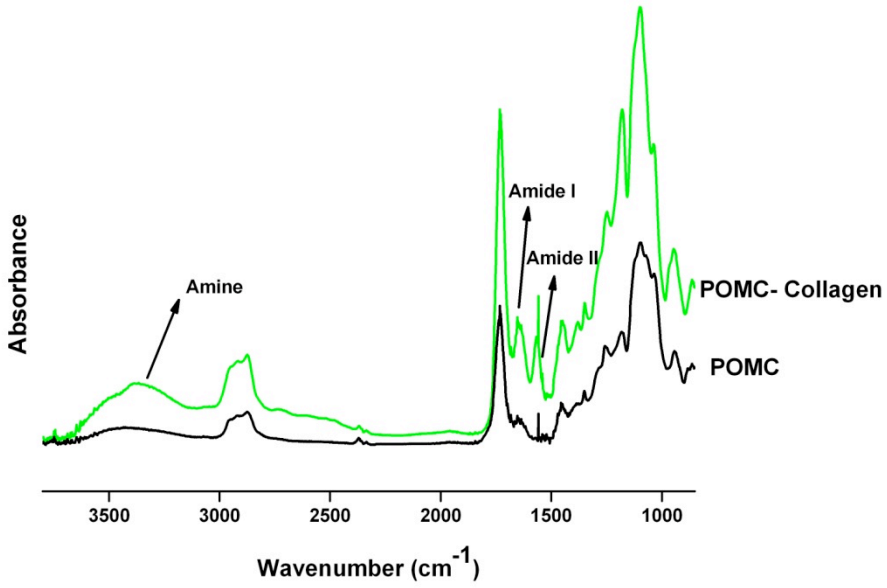

Figure 2.10 ATR-FTIR spectra of POMC 6/4 and collagen modified POMC 6/4 film.

2.3.8 Biocompatibility of POMC

After 72 hours in culture, both HASMCs and NIH-3T3 fibroblast cell lines attached and proliferated on POMC and collagen immobilized POMC films. NIH-3T3 maintained normal and healthy spindle-shape morphology during the proliferation process on both films (Figure 2.11). Quantitative MTT analysis show that cells proliferated better on PLLA films when compared to non-collagen immobilized POMC films. After type-I collagen immobilization, no significant difference in the HASMCs cell adhesion and proliferation was observed for POMC and PLLA films (Figure 2.12).

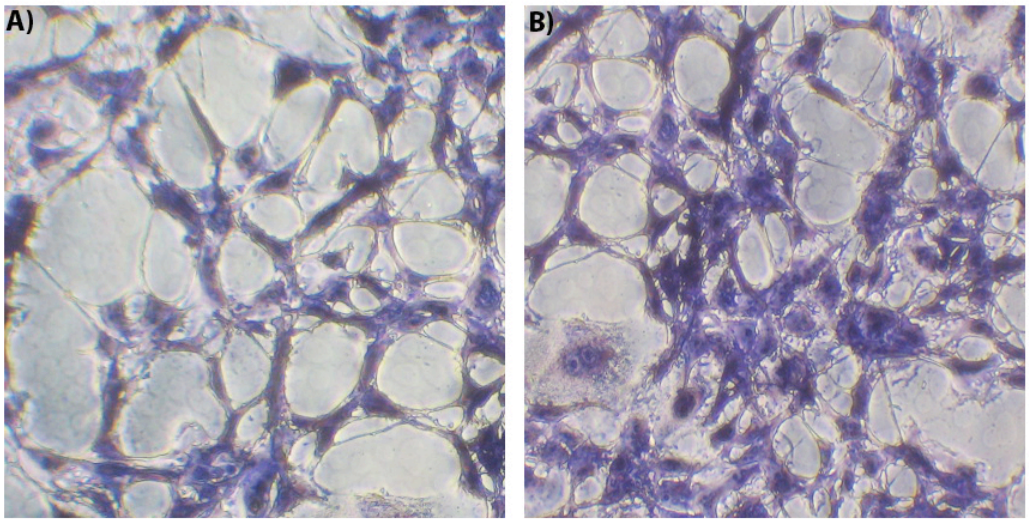

Figure 2.11 A) SEM picture of NIH-3T3 cells culture on POMC 6/4 film and B) collagen immobilized POMC 8/2 film stained with H&E staining.

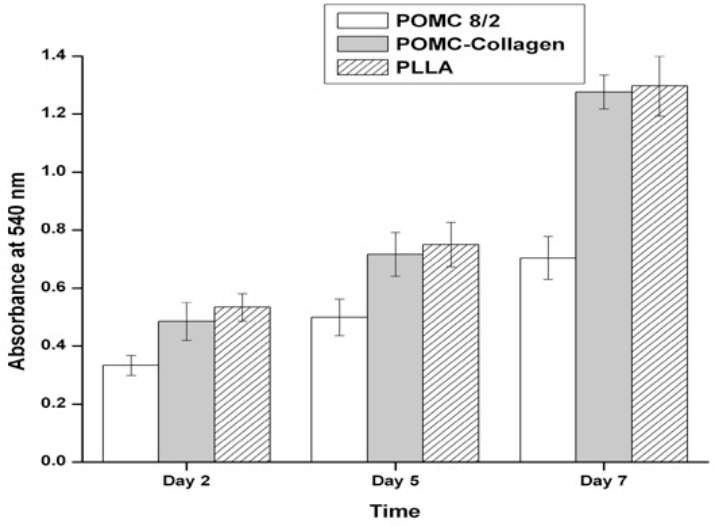

Figure 2.12 Comparison of growth rate of HASMCs on PLLA (control), POMC 8/2 films and collagen modified POMC 8/2 films. MTT absorption was measured at 570 nm. (N = 7).

The foreign body response of POMC was evaluated via subcutaneous implantation in Sprague-Dawley rats. Samples that were implanted for 1 week produced a slight acute inflammatory response (Figure 2.13A), which was expected and consistent with the introduction of foreign materials into body. After 4 weeks of implantation, the number of surrounding cells declined, thus reducing the fibrous capsule surrounding the POMC implant (Figure 2.13B). The

fibrous capsules surrounding the POMC film (176.69±10.19 microns) at week 1 significantly decreased by 19% at week 4 (143.39±8.39 microns), $p<0.001$.

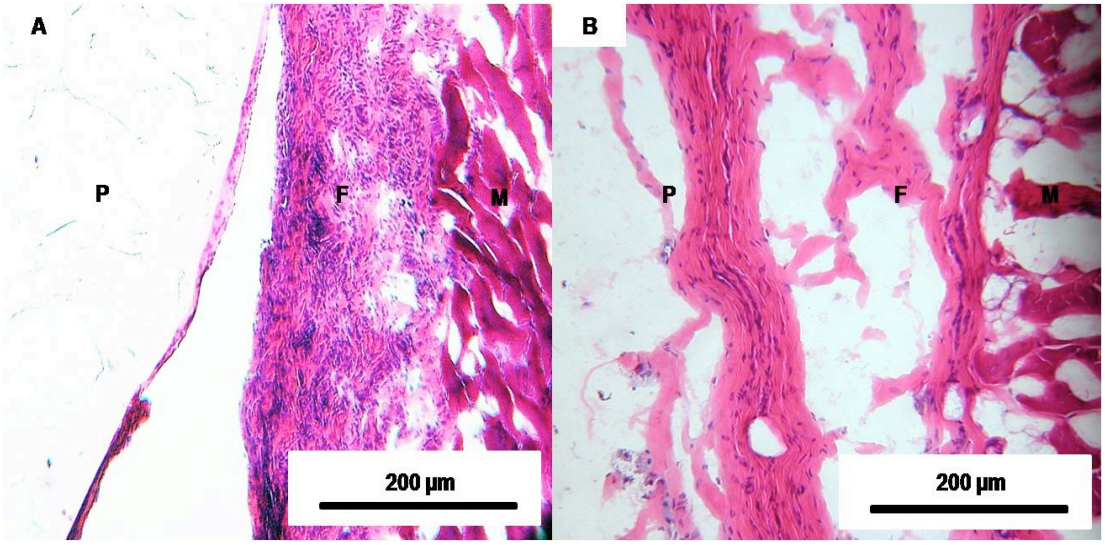

Figure 2.13 Histology of *in vivo* foreign body response of POMC8/2 implanted subcutaneously in Sprague Dawley rats. Impants and surrounding tissues were harvested after A) 1 week; and B) 4 weeks implantation. H&E stain shows reduction of fibrous capsule thickness formed at the implantation when compared for sample of week1 and 4. P, F, and M label polymer, fibrous capsule and muscle respectively.

2.3.9 Micro/Nano Fabrication of POMC

The processability of POMC was demonstrated through the fabrication of micro-porous scaffolds and nanoparticles. Figure 2.14A showed a SEM picture of a cross section of a POMC8/2 scaffold produced by the salt leaching technique. The SEM picture indicated a porous POMC8/2 scaffold. Figure 2.14B showed the POMC8/2 nanoparticles prepared by a solvent displacement method. The average size distribution of the nanoparticles was 65-100 nm.

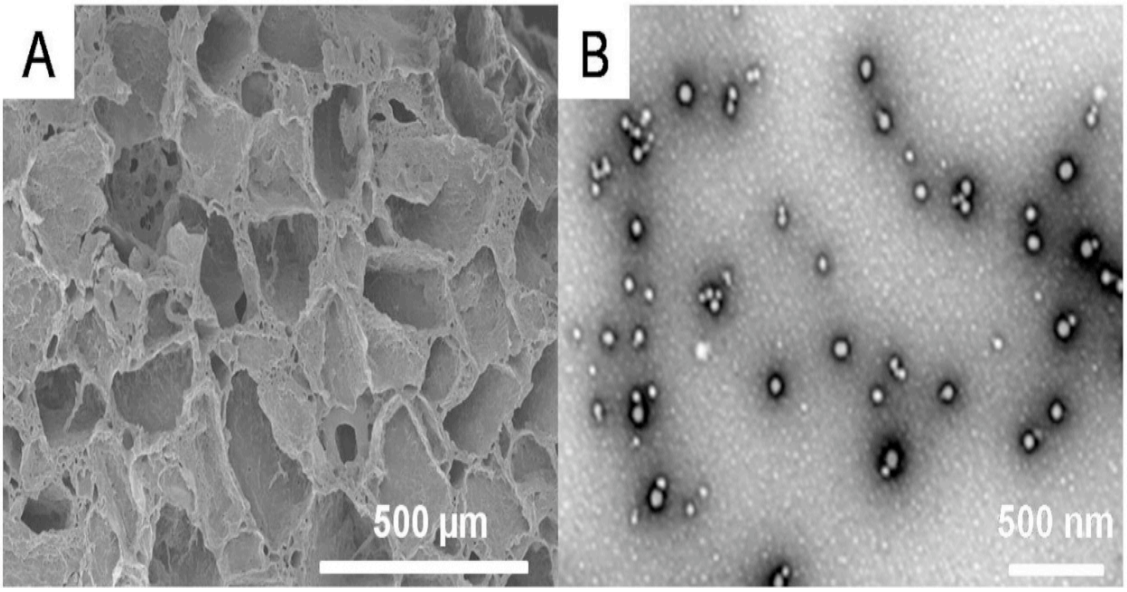

Figure 2.14 A) SEM photograph of POMC8/2 scaffold fabricated by salt-leaching method. B) Transmission electron microscopy (TEM) picture of POMC nanoparticles with particles size in the range of 65-100 nm.

2.3.10 Wound Dressing Formation on Porcine Skin

POMC films adhered perfectly with the skin and can be easily peeled off without sacrificing its integrity (Figure 2.15A-C). The pre-POMCs were in a liquid gel state (Figure 2.15D), and it can be used for *in situ* polymerization without any solvent system. As shown in Figure 2.15D-F, pre-POMC can be easily smeared or injected onto any contour on the skin (Figure 2.15E), and quickly polymerized into a film.

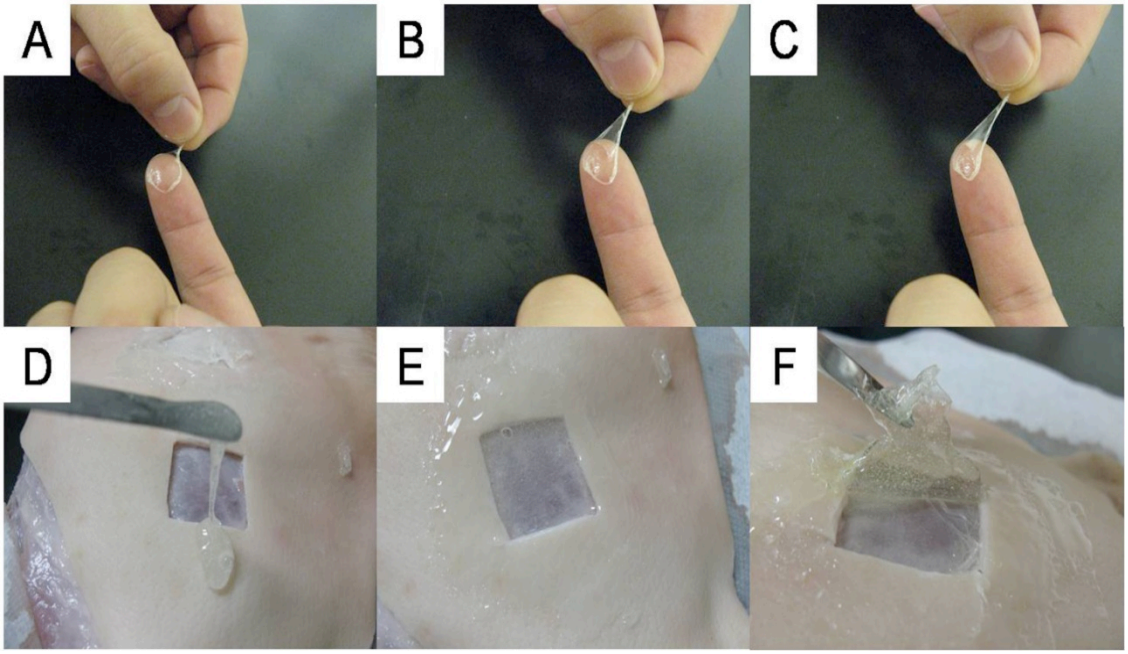

Figure 2.15 A,B) POMC adheres on skin very well C) can be peeled off quickly without sacrificing the film integrity. D) Viscous pre-POMC E) smeared on any contour and F) Crosslinked into film. *In situ* Crosslinking of POMC can be achieved within 3 minutes under 365 nm Ultra Violet light.

2.4 Discussion

Tissue engineering and wound healing are fast-growing fields which place a huge need for suitable biomaterials to solve unmet clinical problems. Until recently, the development of ideal *in situ* rapidly crosslinkable biodegradable biomaterials have been a challenge. The objective of this study was to synthesize and characterize a new *in situ* crosslinkable biodegradable synthetic hydrogel. The importance of matching the scaffold mechanical properties to those of the tissues has been recognized. However, the tunability of the mechanical properties of POC was achieved at the price of sacrificing the functional groups in the pre-polymer backbone, thus limiting its potential for further bioconjugation. In addition, heating is necessary for the crosslinking of POC. To overcome this issue, introducing a vinyl component (maleate) in the backbone of POC would confer the *in situ* crosslinkability to POMCs without heating and sacrificing the available functional groups. This new approach to crosslink the polymer network

will open new windows for broader biomedical applications in which biodegradable elastomers are needed.

The synthesis of POMCs was easy, simple, and inexpensive. The polycondensation reaction between CA, OD, and MA was driven forward by removal of water through the addition of heat. In order to prepare a linear pre-polymer of lower molecular weight, the reaction was subjected to heat for limited amount of time. Induction of maleic acid in the pre-polymer brought in double bonds that can be utilized for the formation of C-C bond via photocrosslinking ultraviolet light. The trifunctional citric acid contributes the excess pendent carboxylic and hydroxyl group in the polymeric backbone. The ester linkages of the polyester polymers confer biodegradability to the polymers(37). The aliphatic diol, 1,8-octanediol was to balance the hydrophobicity/hydrophilicity and participated in the degradable ester bond formation.

The compositions of the polymer determined by ^{1}H NMR were found to be consistent with the feed ratios as seen in Table 1. Thus, all the monomers have participated in the reaction as expected. The ^{1}H NMR also shows two different pair of vinyl hydrogen peaks between 6 and 7 ppm. This suggests that maleic acid has been incorporated into the polymeric chain in two different environments (at the end and at the middle of the chain). This can be explained with the concept of 1st and 2nd acid dissociation constant (pKa) values of both acids. The 1st pKa values of maleic acid and citric acid is 1.97 and 3.15 respectively, and the 2nd pKa values is 6.07 and 4.77 respectively. As both of the acids need to take part in the reaction, the lower 2nd pKa value of the citric acid will become more reactive than the maleic acid. This increases the chance for polymer chain to terminate with maleic acid.

Similarly, the FTIR spectra confirmed the presence of all the characteristic bonds such as ester, double, and hydrogen bonds between hydroxyl group and carbonyl group that contribute to the biocompatibility, hydrophilicity, degradability, thermal and mechanical properties of the materials(93). As compared to the FTIR spectra of the reported POC synthesized from citric acid and 1,8-octanediol,(94) an additional peak at 1650 cm^{-1} of pre-POMC suggested that maleic acid was incorporated in the chain of the pre-polymer. The double bond peak at 1650

cm^{-1} significantly decreases when pre-POMC is subjected to UV crosslinking. The peaks centered at 3750 cm-1 on both pre-polymers and photocrosslinked films indicate the crosslinked polymers still remain significant –COOH and –OH groups which are essential for potential bioconjugation.

The typical DSC thermograph showed the glass transition temperatures (T_g) ranging from -36 to -9.10 °C, without any crystallization and melting peaks, thus maintaining an amorphous state at room or body temperature characteristic for elastomers (95). As the amount of maleic acid increased in the polymers, the T_g of the polymers further decreased. This was due to the presence of isolated double bonds which facilitates polymer to move freely even in lower temperatures. In addition, as the amount of maleic acid increased, the amount of citric acid decreased which reduced the amount of hydrogen bonding that is responsible for polymer chain immobility. The thermograph of TGA confirmed that the polymer decomposes 10% of its mass at temperature of 310 °C to 363 °C. Thus, it can be concluded that this material has better thermal stability and lower T_g than the available elastomer POC. The high decomposition temperature suggested that the POMC should be safe for autoclave sterilization, a common way for biomaterial sterilization. The low T_g of POMCs makes the materials soft and elastic at the common use temperature, body or room temperature.

One of the prime interests in developing such biodegradable elastomers was that the mechanical properties of POMC can match with the desired tissues (92, 93, 95-97) such as myocardium of human (tensile strength: 3-15 kPa; Modulus: 0.02-0.5 MPa) (72), stratum corneum of human skin (breaking threshold of 20-40 kPa) (98) , human bladder (tensile strength: 0.27±0.14 MPa; Modulus: 0.25±0.18 MPa) (93). The mechanical properties of such soft tissues fall within the range of the POMC mechanical properties. The mechanical properties of the PMOC could also be adjusted by varying the choice of monomers, the molar ratio of the monomers, the amount of PI used, and concentration of polymer. For example, very soft and elastic polymers can be achieved by using lower initiator concentrations, lower polymer

concentrations, and higher molar ratios of citric acid; while tough elastomers can be obtained by using higher initiator concentrations, higher polymer concentrations and higher molar ratios of maleic acid. It should be noted that if citric acid is not present in the polymeric network POMC10/0, there is significant decrease in ultimate tensile strength of the polymer. This explains that the strong hydrogen bonding between carboxylic acid and hydroxyl also have some contribution on the strength of the elastomer. In addition, the elastic mechanical properties of the polymer can be further modulated by changing the diol including aliphatic diols such as C2-C12 diols and macrodiols such as poly(ethylene glycol) (PEG) of various molecular weights. The use of PEG for the polymer synthesis can make the polymers water-soluble (data not shown). Thus, the mechanical properties of POMC can be finely tuned to match those of soft tissues in the body.

The degree of swelling in all three different swelling agents showed a trend that the higher the maleic acid incorporated in the polymer chain, the lower the swelling capability of the polymer. It should be noted that a dramatic change in the swelling ratio in PBS (pH 7.4) and water (pH 7.0) suggest that these pendent carboxylic acids were deprotonated and ionized in a higher pH thus repelling the polymer chains from each other and therefore permitting higher amounts of swelling agent to enter inside the networks. Furthermore, the swelling capability of the polymer in DMSO was also affected by concentration of PI and polymer used while crosslinking whereas these conditions had no effect on water uptake capability of the polymer. The lower swelling ratio observed by higher PI concentration could be explained due to the fact that high amount of initiator create high crosslinking degree of the polymer networks. Similarly, a higher swelling ratio observed with a lower polymer concentration while crosslinking was due to the fact that when the polymer concentration was high, there was a high chance of forming intermolecular crosslinking, whereas a lower polymer concentration subjected the polymers to a higher chance in intramolecular crosslinking. This property also contributed for the elastic properties of the elastomer. Furthermore, only increasing the amount of citric acid enhances the water uptaking ability of the polymer. This is because higher amount of citric acid increase the amount of

carbonyl and hydroxyl group that increase the hydrophilicity of the polymer. The swelling ratio should have direct relation with the degree of crosslinking and the properties of the building blocks of the polymeric network. The swelling results suggest that the degree of crosslinking of POMC can be controlled according to the requirement of specific applications.

The degradability of the POMC was evaluated by incubating polymer film in PBS at 37 °C over a 3-month period. It was observed that as the amount of citric acid increased, the degradation rate increased. This is due to the fact that citric acid increased the hydrophilicity of the polymer. The PBS swelling studies also supports this phenomenon. The polymer uptakes more fluid as the amount of citric acid increases, thus creating more chances for the ester bond to be degraded by hydrolysis.

A preliminary biocompatibility evaluation was done with POMC8/2 films *in vitro* and *in vivo*. It was observed that and 3T3 fibroblasts display typical spindle-shape morphology on POMC films and collagen modified POMC film. When implanted *in vivo*, the polymers did not trigger edema and tissue necrosis on all the tested animals. Although, a slight acute inflammation response was observed in the 1st week of the implantation, the number of surrounding cells declined reducing the fibrous capsule around the sample at 4th week implant. This clearly suggested that degradation products of POMCs were not toxic. The preliminary *in vitro* and *in vivo* biocompatibility evaluation suggested that POMCs are biocompatible materials. However, detailed biocompatibility tests of POMC will be the topic of future publications.

One major benefit of POMC is that the polymer remains saturated with pendant functionalities after *in* situ crosslinking. Cellular adhesion and proliferation on unmodified POMC films produced poor results, which could be expected from the functionally rich surface of the material and is similar to the results of other studies (40). However, type I collagen modified POMC films showed a significant increase in the cellular proliferation, and was comparable to the cellular response on PLLA films. Unlike previous elastomers, no further post-modifications are required to introduce functional groups, which may alter the properties of the material. In addition, the conjugation for POMC is simple and can be performed in the bulk of the material. Thus, the

conjugation could potentially have a longer lasting effect than previous modification methods. (99) The unreacted carboxylic acid and hydroxyl groups on the POMC backbone can potentially be used as bioconjugation sites if proteins,(100-102) drugs, peptides (103), and ligands (104) are needed to confer biological functions to the materials.

The processability of POMC was demonstrated by the fabrication of micro-porous 3-dimensional scaffolds and nanoparticles. The pre-POMC was soluble in a wide range of organic solvents such as acetone, 1, 4-dioxane, DMSO, DMF, and THF thus they could be processed as many other polymers for micro/nano-fabrications. The photocrosslinking of pre-POMC can be completed within 3 minutes, which is much shorter than many other existed photocrosslinkable polymers that normally require at least 10 minutes of photopolymerization. We have demonstrated that POMC could be fabricated into a 3-dimensional tissue engineering scaffold using the commonly used particulate leaching technique. Nanoparticles with the particular size of around 100 nm could be easily fabricated from POMC and can potentially be loaded with drugs or further conjugated with ligands and antibodies for targeted drug delivery application because the photocrosslinking does not sacrifice the available functional –COOH and –OH groups on the polymer backbone.

POMC can potentially be used an ideal wound dressing materials. In the US, the direct cost of wound dressing is estimated to be more than $5 billion per year. A significant number of soldiers are evacuated from battlefield because of severe burn injuries. Skin wounds are less severe than the large burns, but can potentially result in the temporary loss of soldiers from their unit. Despite the advances in burn care, the mortality rate of wound injuries continues to be high. The ideal wound dressing should meet the following requirements: 1) convenience for uses; 2) conformability, particularly with uneven body surface; 3) absence of antigencity and toxicity; 4) mechanical stability and compliance; 5) control of fluid loss and infection; 6) cost-effectiveness and availability; (105, 106) However, none of the current wound dressings/barriers or bandages can meet all the above requirements for wound treatment. A soft, elastic, tough,

biocompatible, rapidly *in situ* forming hydrogel may potentially address the shortage of ideal wound dressing materials for wound care.

The short photopolymerization time makes the POMC hydrogel more practical for *in situ* applications than other current hydrogels. As we have mentioned earlier, pre-POMC can be made into water-soluble when PEG was used as the diol or part of the diols for polymer synthesis. In addition, pre-POMC itself was also gel-like liquid which allowed an *in situ* polymerization under UV crosslinking. Thus, POMC should be well suitable for *in situ* applications. We have preliminarily demonstrated the potentials of using POMC as a rapidly forming and fast peeling wound dressing materials. There are potential two ways to use POMC as wound dressing materials. POMC can be prefabricated into films which could be well adhere to the skin and could be fast-peeled off without destructing the integrity of the films (Figure 2.15A-C). In addition, the gel-like pre-POMC can potentially act as a liquid bandage/dressing which may easily be smeared or dropped on the skin (Figure 2.15D-F) with any contour just like using toothpaste and quickly photopolymerized to form a film or gel *in situ* with potential drugs encapsulated if needed. Since POMC has tunable degradability, it can potentially be absorbed on the skin when its mission is completed or can be disposed of without polluting the environment. Furthermore the transparent nature of POMC could potentially allow monitoring the wound healing process visually if needed.

2.5 Conclusion

In this work, we have synthesized and evaluated a new class of synthetic biodegradable elastomeric polyester hydrogel, POMC, which can be crosslinked *in situ* within a short period of time. Preliminary biocompatibility of POMC was evaluated by smooth muscle cell and fibroblast cell culture and subcutaneous implantation in rats. POMC possess great processability, excellent biocompatibility *in vitro* and *in vivo*, and tunable degradability and mechanical properties. POMC can potentially be a platform biomaterial for various biomaterial derivatives. The development of POMC should expand the choices of available biomaterials for a broad range of biomedical applications.

CHAPTER 3

POLY(POLY (ETHYLENE GLYCOL) MALEATE CITRATE) (PPEGMC)

3.1 Introduction

POMC holds great potential as an injectable tissue engineering scaffolding material. In addition to the tunable properties, the available hydroxyl and carboxylic groups can be used for bioconjugation or other surface modifications. Its mild crosslinking strategy allows for the encapsulation of temperature sensitive biomolecules and cells. Although POMC is viscous in its pre-polymeric state to serve as an injectable polymer, its properties are better tuned while in a solvent solution while crosslinking. It was observed that POMC is soluble in wide range of solvent including chloroform, tetrahydrofuran, dichloromethane, acetone, dimethylformamide, 1,4-dioxane, and dimethyl sulfoxide, but has poor solubility in water. POC shows poor hydrophilicity due to the hydrophobic constituent, 1,8-octanediol, which was supported by the low water uptake and slow degradation profile. These properties are desirable for tissue engineering scaffolds, but adversely affect in the performance of a delivery vehicle. By replacing the diol with a very hydrophilic macrodiol such as poly(ethylene glycol), PPEGMC should perform as an excellent delivery vehicle. Furthermore, PPEGMC can also be crosslinked into nanoparticles and microparticles with pendent carboxylic and hydroxyl groups for conjugation of biomolecules such as ligands and antibiotics for site-specific application.

This new class of synthetic, elastomeric, and biodegradable polyester is composed of poly(ethylene glycol) (PEG), maleic acid (MA), and citric acid (CA), which have all been used in numerous biomedical applications. Structural analysis, mechanical, swelling ability, sol content, cell encapsulation, degradation, drug release profile, cytotoxicity of degraded products, and the

processability of the hydrogel have been thoroughly investigated in order to meet the specific requirements to serve as a drugs/cells delivery vehicle.

3.2 Materials and Methods

3.2.1 Materials

All chemicals, cell culture medium and supplements were purchased from Sigma-Aldrich (St. Louis, MO), except where mentioned otherwise. All chemicals were used as received.

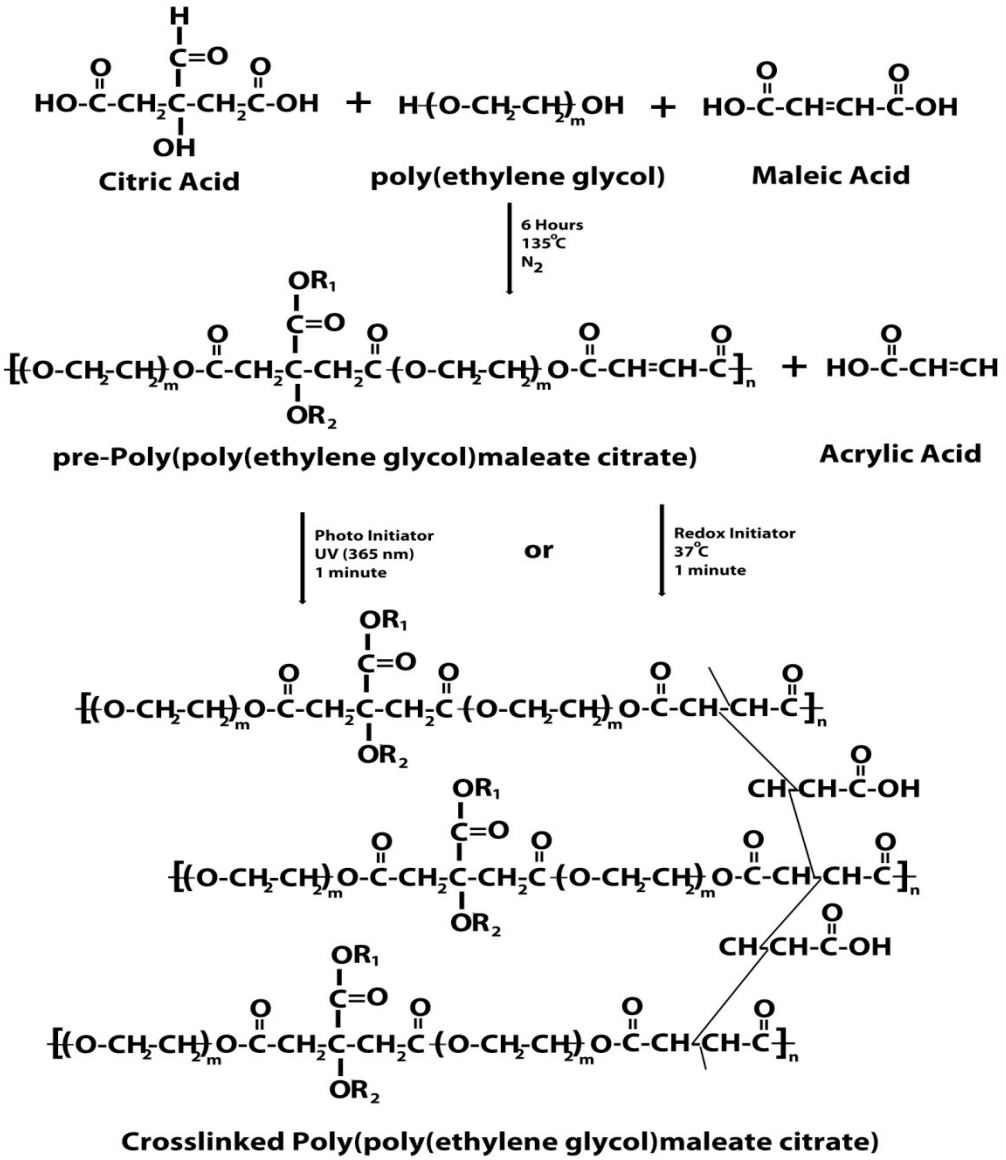

Figure 3.1 Synthesis Scheme of PPEGMC. The synthetic scheme comprise following steps: 1) Synthesis of pre-PPEGMC incorporating the following monomers: a multifunctional (carboxylic acid) Citric Acid, Vinyl functional Maleic Acid, Alcohol containing Poly(ethylene glycol). Ratios of Maleic Acid and Citric Acid were varied as 8/2, 6/4, and 4/6 respectively, where as ratio of overall acid to alcohol was kept as 1:1. All the monomers were melted at 160 °C under nitrogen blanket. Further polymerization was continued at 135 °C to achieve low molecular weight pre-polymer. PPEGMC can be crosslinked with crosslinker (Acrylic Acid) either under 365 nm ultraviolet light for 1 minutes in presence of photoinitiator (2,2'-Azobis(2-methylpropionamidine)dihydrochloride) or at 37 °C in presence of redox initiator system (Ammonium per sulfate and Ascorbic acid). R_1 can be PEG or hydrogen and R_2 can be citric acid, maleic acid and hydrogen.

3.2.2 Synthesis of Pre-PPEGMC

All the chemicals were purchased from Sigma-Aldrich (Milwaukee, WI) and used as received. The formulation of PPEGMC pre-polymer was synthesized as described in the schematic in Figure 3.1. CA, PEG, and MA were melted in a 250 mL three-necked round bottom flask fitted with an inlet adapter and outlet adapter for first 20 minutes by stirring the contents in the flask at a temperature of 160 °C under nitrogen gas flow. Once the constituents melted, the temperature was reduced to 130 °C for 2 hours. The pressure was then dropped to 50 mTorr for another 2 hours. Finally, the reaction was the left at ambient pressure and closely watched until desired viscosity was achieved. The prepared prepolymer was dissolved in deionized water and dialyzed with 500 Da cut off molecular weight membrane for 3 days. This was followed by lyophilization to achieve a pure form of pre-PPEGMC. Different ratio of acids, maleic acid, and citric acid, were altered in the initial composition of the pre-polymer as 8/2, 6/4, and 4/6 respectively as shown in Table 1. However, the overall ratio of the acids over the diol was kept as 1:1.

Table 3.1 Feeding ratio and actual composition of pre-PPEGMC**.**

Polymer Name	MA:CA:OD (moles)	Feeding Ratio MA:CA:OD	Composition MA:CA:OD
PPEGMC 8/2	0.08/0.02/0.10	0.4/0.1/0.50	0.37/0.12/0.50
PPEGMC 6/4	0.06/0.04/0.10	0.3/0.2/0.50	0.28/0.2/0.52
PPEGMC 4/6	0.04/0.06/0.10	0.2/0.3/0.50	0.17/0.31/0.48

3.2.3 Characterization of Pre-PPEGMC

To analyze the functional groups present in the pre-polymers, a 5% pre-PPEGMC solution in 1,4-dioxane was smeared on a potassium bromide crystal and dried overnight in a vacuum hood. Fourier Transform Infra Red (FT-IR) spectroscopy measurements were recorded at room temperature using a Nicolet 6700 FT-IR (Thermo Scientific, Waltham, MA) equipped with OMNIC Software using 64 scans across the wave numbers 4000 - 400 cm^{-1} at a resolution

of 2 cm^{-1}. Similarly, the pre-polymers were purified twice as mentioned above and then dissolved in dimethyl sulfoxide-d_6 (DMSO-d_6) to make a 3% pre-polymer solution and placed inside a 5-mm-outside diameter tube. Proton Nuclear Magnetic Resonance (^{1}H NMR) was used for the analysis of the actual composition of the PPEGMC pre-polymers for all ratios on 250 MHz JNM ECS 300 (JEOL, Tokyo, Japan). The chemical shifts for the ^{1}H-NMR spectra were recorded in parts per million (ppm), and were referenced relative to tetramethylsilane (TMS, 0.00 ppm) as the internal reference.

3.2.4 Preparation and Characterization of PPEGMC Hydrogel

Pre-PPEGMC was crosslinked by free radical polymerization. The purified pre-polymer was dissolved in water to make a 30% polymer by weight concentration. Acrylic acid was used as crosslinker and 2,2'-Azobis(2-methylpropionamidine)dihydrochloride was used as photoinitiator. In this study, the percentage of photoinitiator was fixed as 0.30% (w/w) with the polymer solution where as the concentration of crosslinker was varied as 3-9% to study the effect of crosslinker in the overall hydrogel performance. Next, the solution was poured into a Teflon mold and placed under a UVP 365 nm Long Wave Ultraviolet Lamp (Upland, CA) for 60 seconds. The photocured hydrogel achieved through this process is also represented by schematic in Figure 1. Bond vibrations of crosslinked film of PPEGMC were evaluated using FTIR and compared that of pre-polymer.

3.2.5 Mechanical Properties of PPEGMC Hydrogel

The tensile mechanical properties were studied according to the ASTM D412a standard on an MTS Insight II mechanical tester equipped with a 500 N load cell (MTS, Eden Prairie, MN). Crosslinked and freeze-dried PPEGMC films were cut using a dog bone shaped (26 mm × 4 mm × 1.5 mm; length × width × thickness) aluminum die. The dog bone shaped films were pulled until failure at a rate of 500 mm/min to obtain the stress strain curves. The initial slope (0-10%) of the curve was used to determine the modulus of the material. A detailed study on the effect of different ratios of the monomers, and the amount of crosslinker on mechanical properties of the polymer was performed.

3.2.6 Swelling Ratio and Sol Content Measurements

Purified PPEGMC was fabricated according to the process mentioned above. PBS, deionized water, and buffer solutions of different pH (2.4, 3.4, 4.4, 5.4, 6.4, 8.4, 9.4, 10.4) were used as the swelling agents in this study. Six discs of 4 mm in diameter were allowed to swell in the respective swelling agents until the equilibrium state was achieved (2 days). The surface of the swollen discs was gently blotted with filter paper to remove any excess swelling agent, and the sample was then weighed (M_w). The discs were freeze-dried for 3 days and weighed to determine the dry weight (M_d). Equation 1 calculated the equilibrium-swelling ratio.

For sol gel fraction measurement, crosslinked films were freeze-dried prior to purification and weighed to find the initial mass (M_i), and suspended in fresh dioxane every six hours for twenty-four hours and followed by freeze-dried for seventy-two hours. The dried samples, absent of non crosslinked pre-polymer, were weighed to obtain (M_d). The sol gel fraction (SFG%) was calculated by Equation 2.

Both the experiments were repeated three times and the average value was reported. The effects of MA/CA ratio in the polymer chain and crosslinker concentration in the network on swelling ratio and sol gel fraction were also evaluated in this experiment.

$$\text{swelling}\,(\%) = \frac{W_s - W_d}{W_s} \times 100 \qquad (1)$$

$$\text{sol}\ (\%) = \frac{W_i - W_d}{W_i} \times 100 \qquad (2)$$

3.2.7 In Vitro Degradation Study

Six polymer discs (4 mm in diameter) were cut from the purified crosslinked films using a cork borer. The discs were weighed to find the initial mass (M_i), and suspended in PBS (pH 7.4), and maintained at 37 °C. The pH was monitored and the buffer was replaced every day for first week and every subsequent week to ensure a constant pH of 7.4. At the desired time point,

the samples were rinsed with deionized water, freeze-dried, and weighed to find the remaining mass (M_t). Photographs with a Hitachi S-3000N scanning electron microscope (Hitachi, Pleasanton, CA) were taken to understand the morphology of the degraded network. The percent mass loss (%ML) was calculated by Equation 3.

$$\text{Mass Loss} \quad (\%) = \frac{M_i - M_t}{M_i} \times 100 \qquad (3)$$

3.2.8 Drug Loading and In Vitro Release

BSA was chosen as the model drug for the controlled release study. A BSA solution was first prepared by dissolving 2.0 g of BSA in 40 mL of PBS solution (pH 7.4). Then, the appropriate amount of the drug solution was mixed with the polymer solution to make a 1:20 drug to polymer ratio. The in vitro release was carried out at 37 °C to investigate the effect of the pH sensitivity of the PPEGMC hydrogel on protein release profiles. BSA release study was performed by immersing the above BSA-loaded hydrogel sample in a glass bottle filled with a 10 mL of buffer solution (pH 7.4) and buffer solution (pH 2.4). At a predetermined period, BSA released buffer solution was removed from the glass tube and hydrogel was placed in a fresh 10 ml of buffer solution. The concentration of the BSA was measured by using a UV spectrophotometer at 280 nm. The results were presented in terms of cumulative release as a function of time, and the cumulative BSA release (%) was calculated as shown in equation 4, where M_t is the amount of BSA released from the hydrogel at time t and M_o is initial BSA loaded in the hydrogel.

$$\text{Cumulative Release} \ (\%) = \frac{W_t}{W_o} \times 100$$

3.2.9 PPEGMC Scaffold Fabrication

Scaffold fabrication was done using gas foaming technique. Briefly, PPEGMC pre polymer was mixed with 6% crosslinker, 0.3% photoinitiator and dissolved in DI water to make 30% (w/w) polymer solution. Then 1% of calcium bicarbonate was added to the solution as a gas foaming agent just prior to crosslinking with UV light. The scaffolds obtained were freeze-

dried for 48 hours to remove all traces of water. The scaffold was then freeze fractured using liquid nitrogen, and the cross section of the fractured sample was examined under a Hitachi S-3000N scanning electron microscope (Hitachi, Pleasanton, CA).

3.2.10 In Vitro Cell Surface Attachment and Encapsulation

PPEGMC 6/4 was used for all cytocompatibility evaluation studies. Photocrosslinked PPEGMC film were cut into discs (4 mm diameter), sterilized in 100% ethanol for 30 minutes, and placed under UV light for another 30 minutes. NIH 3T3 fibroblasts (ATCC) were used as model cells for this study. The cells were cultured in Dulbecco's modified eagle's medium (DMEM), which had been supplemented with 10% fetal bovine serum (FBS) and 1% penicillin streptomycin. The culture flasks were kept in an incubator maintained at 37 °C, 5% CO_2, and 95% relative humidity. The cells were allowed to grow to the fourth passage, trypsinized, centrifuged, and suspended into media to obtain a seeding density of 1×10^5 cells/ml. Then, cells were seeded on top of the film using static seeding technique. The cells on the film were allowed to proliferate in Dulbecco's modified eagle's medium (DMEM) with 10% fetal bovine serum (FBS) for 3 days in an incubator maintained at 37°C, 5% CO_2 and 95% humidity. The cells were then fixed in 5 ml of 2.5% (w/v) gluteraldehyde-PBS solution, and observed under an inverted microscope (Zeiss Auxiovert).

For the purpose of cell encapsulation study, immediately prior to the trypsin treatment, 3T3 fibroblasts were labeled with carboxyfluorescein diacetate, succinimidyl ester (CFDA-SE) green fluorescent cell tracer using the manufacturer's protocol. Pre-polymer solution (30% w/w) in deionized with 3% crosslinker and 3% lysine was mixed thoroughly and filtered out with 0.2 um syringe. Simultaneously, 0.3% of photoinitiator (w/w) to the polymer solution was dissolved in DI water and filtered through 0.2 um filter. A one million cells per ml suspension was mixed thoroughly with polymer solution and poured into 96 well plates. Prior to photo radiation with 365 nm UV rays, photoinitiator was mixed thoroughly with polymer-cell suspension. The final solution was allowed to crosslinked for 120 seconds. These cell embedded hydrogel constructs were quickly moved to 24 well plate and suspended in DMEM media for 24 h of time period.

Photographs of cells encapsulated inside PPEGMC hydrogels were taken after the polymerization and after 24 h in DMEM media for further analysis.

3.2.11 Statistical Methods

All the experiments were repeated three times and the average value was reported. Data are expressed as mean ± standard deviation. Statistical analysis was performed using one way-ANOVA with post hoc Neuman–Keuls testing to ensure that groups are statistically different. The swelling data and mechanical properties of the polymer were compared with one way ANOVA. Data were taken to be significant, when a p-value of 0.05 or less was obtained.

3.3 Results and Discussion

3.3.1 Chemical Characterization of Pre-PPEGMC

The PPEGMC pre-polymers formed after the initial controlled polymerization step (Figure 3.1) consisted of a transparent viscous fluid. The pre-PPEGMC is soluble in most of the organic solvent such as dimethylformamide, tetrahydrofuran, chloroform, 1,4-dioxane, acetone, dichloromethane, dimethyl sulfoxide, and water. The presence of carbonyl group (1710-1750 cm^{-1}) from esters and carboxylic acids, hydroxyl group (3100-3600 cm^{-1}) from carboxylic acid and free hydroxyl group , methylene (2700 cm^{-1}), and vinyl group (1647 cm^{-1}) were determined from FT-IR data present in Figure 3.2.

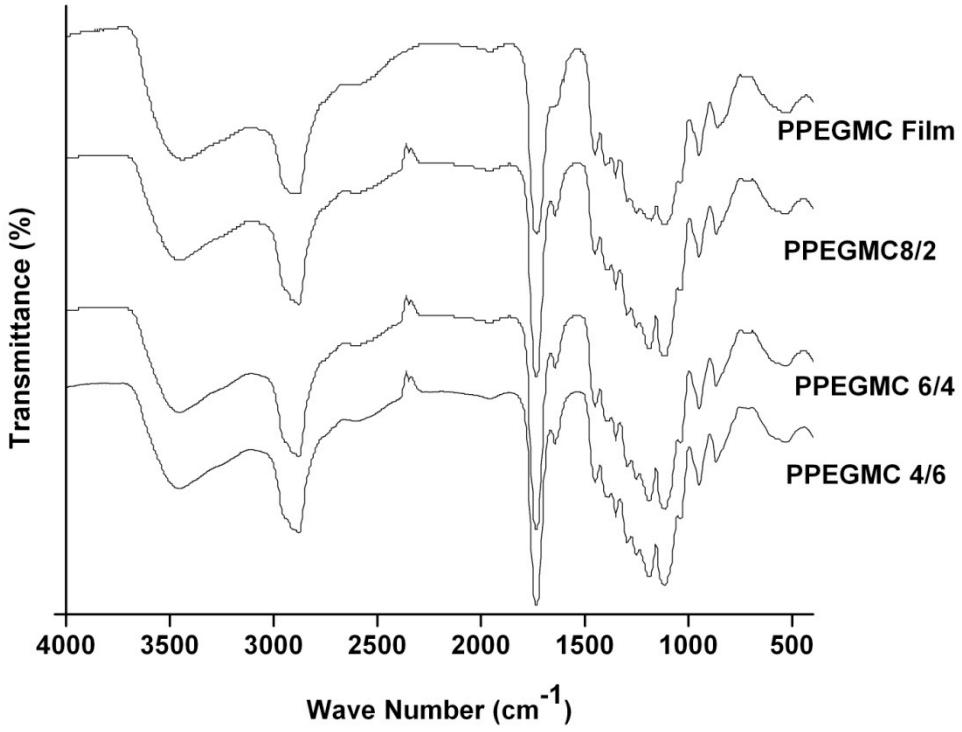

Figure 3.2 FT-IR spectra of pre-PPEGMC and photocured PPEGMC.

Various hydrogen resonances present in the pre-PPEGMC were confirmed by the corresponding chemical shift of ^{1}H-NMR peaks correlated with TMS. As shown in figure 3.3, a typical spectrum of pre-PPEGMC 6/4, the peaks of vinyl functionality (a) of polymeric chain appeared at 6.12 and 5.89 ppm, methylene group (b) at 2.79 ppm, hydroxyl groups (e and f), and the peaks of methylene groups (c and d). The pre-PPEGMCs were also designed to have various molar ratios of citric acid and maleic acid (8/2, 6/4, 4/6) whereas the overall molar ratio of acids to the macrodiol was fixed at 1:1. The area under the characteristic proton peaks from maleic acid (a/2), citric acid (b/4) and PEG (c/2) were integrated and compared to the feeding ratio of the monomers. As seen in table 3.1, the ratios of the constituents of the pre-PPEGMCs were in close agreement with the initial feeding ratio of monomers. It should be noted that various chemical shift of vinyl hydrogens were observed in ^{1}H-NMR spectra. Peaks located at

6.12 and 5.89 should be from vinyl hydrogens located in two different environment of the chain as reported elsewhere (107). Similarly, the existence of more than one peak at each location unlike ^{1}H-NMR spectra of pure maleic acid suggests its successful incorporation in the polymer chain.

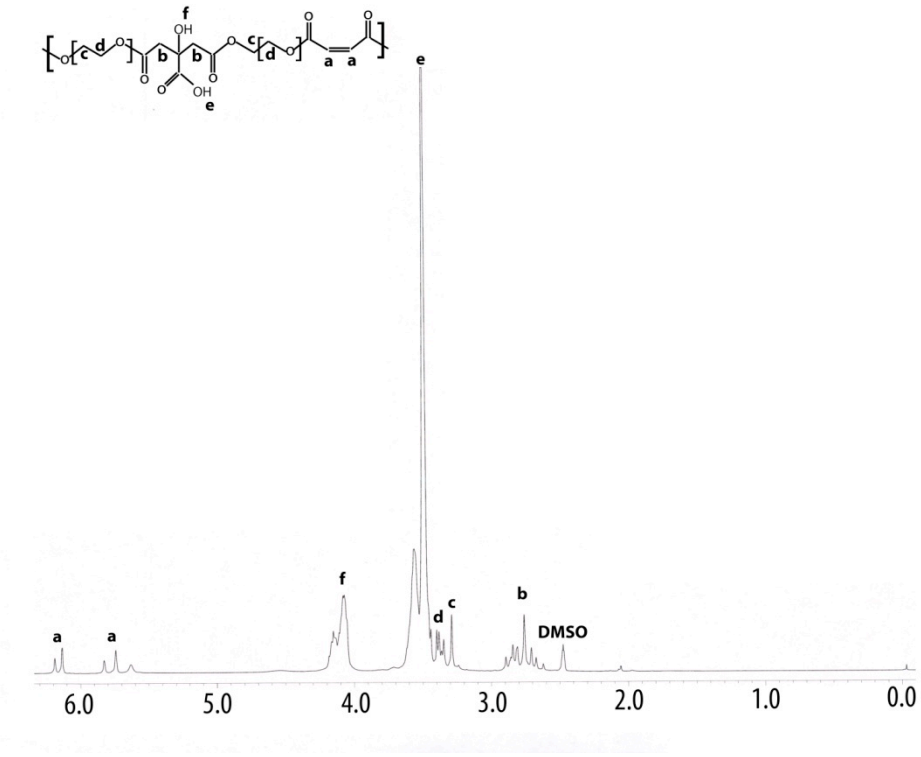

Figure 3.3 A typical ^{1}H-NMR spectrum of PPEGMC 6/4 pre-polymer.

3.3.2 Structural and Physiochemical Characterization of PPEGMC Hydrogel

Crosslinking of the hydrogel network can be achieved by photocrosslinking as well as redox crosslinking mechanism. However, all the characterizations of the polymer in this study are performed on photocrosslinked film in presence of 2,2'-Azobis(2-methylpropionamidine)di-hydrochloride as a photoinitiator and acrylic acid as a crosslinker within 60 seconds of time under 365 nm long wave (Figure 3.1). All crosslinked hydrogels formed are transparent in nature and cannot be dissolved by any types of solvent system. The crosslinking of PPEGMC

was achieved solely by consuming the vinyl moieties in the polymeric chain. This was confirmed by the significant reduction of the shoulder peak at 1647 cm^{-1} in the film that was once present in its polymeric state (Figure 3.2). On the other hand, functionalities such as pendent carboxylic acid and hydroxyl moieties were all well preserved while crosslinking as seen in figure 3.2.

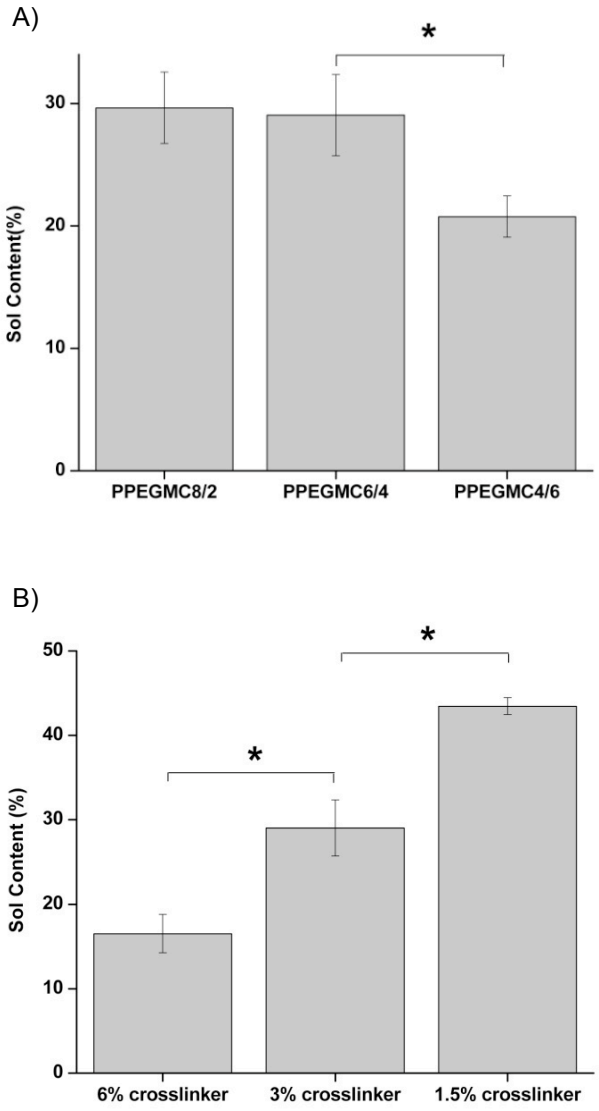

Figure 3.4 Sol-Gel content of the Photocrosslinked PPEGMC hydrogel. A) Effect of MA/CA ratio. B) Effect of crosslinker concentration in the polymer solution while crosslinking (n=6, $p<0.001$).

As seen in figure 3,4, the sol content of the hydrogel depends on the amount of vinyl functionality available in polymer solution either in polymer chain or in crosslinker. As, the amount of vinyl group increases in the polymer chain (due to increase molar of maleic acid), the sol content tends to increase. Although there was no significant difference in the sol content of PPEGMC8/2 (29.64±2.90) and PPEGMC6/4 (29.03±3.32), the sol content was significantly reduced for PPEGMC 4/6 (20.75±1.69) (Figure 3.4a, $p<0.01$). It should be noted that constant concentration (3%) of crosslinker was used to crosslink all three polymers. When crosslinking PPEGMC4/6, as it contained the lowest amount of vinyl groups in the pre-polymer chains, there is an increased chance for more chains to participate in the crosslinking forming more intermolecular crosslinking to decrease the sol content. Whereas crosslinking PPEGMC8/2 and PPEGMC6/4, as they contain higher amounts of vinyl group in one pre-polymer chain, increases the chance of intramolecular crosslinking of the polymer chains resulting in the higher sol content. In contrast, if the vinyl moieties are increased, which was done through the addition of a crosslinker, there is a significant decrease in the sol content of the hydrogels (Figure 3.4b, $p<0.01$). For example, if 1.5% of crosslinker was used to crosslink PPEGMC6/4, sol content was as high as 43.46±0.99. If 3% and 6% crosslinker are used to crosslinked the same polymer, the sol content was reduced to 29.03±3.32 and 16.52±2.27 respectively. Thus, it can be concluded that vinyl group of the crosslinker plays significant role in the network formation of the PPEGMC hydrogels.

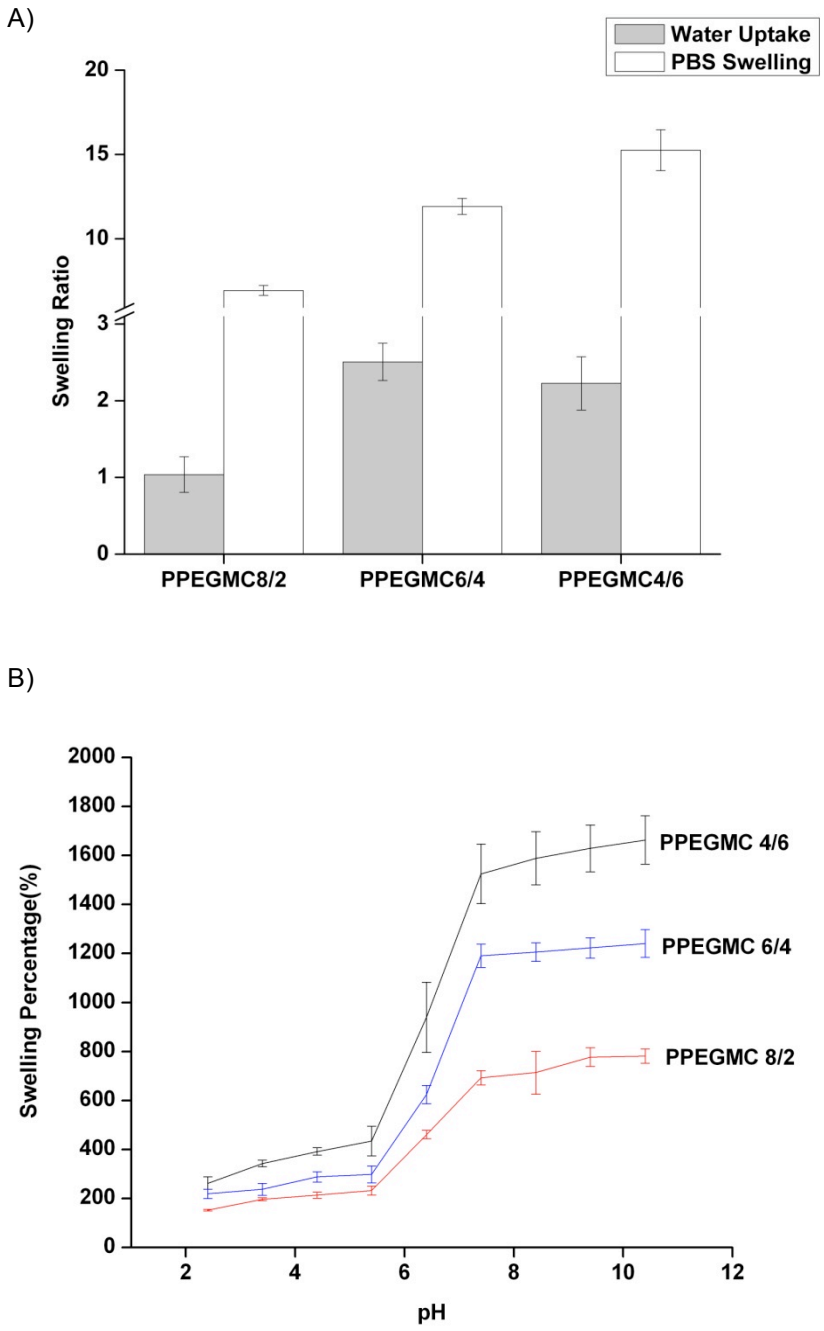

Figure 3.5 Swelling Ratio of PPEGMC hydrogels with different MA/CA ratios. A) In water and PBS. B) in different pH of the swelling agent. Buffer solution of different (pH 2.4, 3.4, 4.4, 5.4, 6.4, 7.4, 8.4, 9.4, and 10.4) were used as swelling agent (n=6).

The swelling ratios of PPEGMC hydrogels crosslinked with various conditions were calculated by comparing the weight changes of the network at fully hydrated conditions and after drying. Figure 3.5a shows the effect of molar ratio of MA and CA on swelling ratio of PPEGMC hydrogels. The results show that the degree of swelling of the hydrogels when crosslinked with 3% crosslinker sufficiently increased from 6.92±0.29 to 15.25±1.21 as amount of maleic acid decreased in its composition (PBS). However, the swelling was restricted 5 fold below these values when water was used as a swelling agent for the respective hydrogels. There was a significant increase in the water uptake from PPEGMC8/2 (1.04±0.23) to PPEGMC6/4 (2.50±0.24), but no significant difference for PPEGMC6/4 and PPEGMC4/6 (2.23±0.35). When incubated in water, the mass swelling was further improved in higher citric acid containing networks such as PPEGMC6/4 and PPEGMC4/6 due to hydrophilic nature of the polymer. However, drastic changes in the swelling ability were observed when incubated in PBS. This clearly demonstrates that pendent carboxylic acids of the network are liable for restricting the swelling ability of the polymer in water. Whereas, if PPEGMCs are allowed to swell in PBS, deprotonation of these carboxylic acid occurs resulting in breaking strong hydrogen bonds and creating electrostatic repulsion among chains.

This was also supported by the swelling study data of PPEGMC networks when swollen in media of various pH. For example, the swelling percentage of PPEGMC4/6, PPEGMC 6/4, and PPEGMC8/2 were 262.11±25.37, 219.05±18.50, and 152.36±3.96 respectively at pH 2.4. No significant differences in the swelling percentiles were observed until the pH of the swelling media was increased to 5.4. Interestingly, drastic increase in the swelling ability of all three networks was observed between 5.4 to 7.4 pH. Finally, all PPEGMCs show a constant swelling in alkaline media with pH ranging from 7.4 to 10.4 (figure 3.5b). It should be noted from the figure 6, that the effect of pH of the swelling media was the most remarkable for PPEGMC4/6. This could be explained by the fact that PPEGMC4/6 is the polymer network with highest amount of carboxylic acid contributed by critic acid, and a lower crosslinking density due to decreased amount of vinyl moieties contributed by maleic acid.

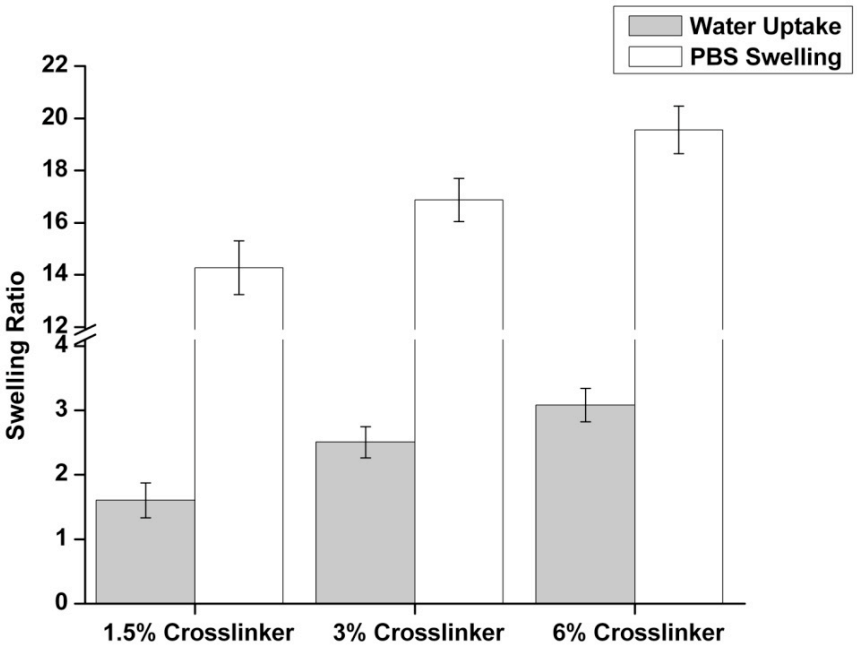

Figure 3.6 Swelling Ratio of PPEGMC6/4 hydrogel in water and PBS, when crosslinked with 1.5, 3, and 6% of crosslinker.

Figure 3.6 shows the effect of the acrylic acid concentration as a crosslinker on the swelling ratio of PPEGMC6/4. For instance, swelling on PBS was increase from 8.28±1.03 to 19.55±0.91 when the crosslinker was increase from 1.5 w% to 6 w%, whereas, water uptaking ability was limited to 1.60247±0.27, 2.51±0.24, and 3.08±0.26 for 1.5 w%, 3w%, and 6w% of crosslinker respectively. Although, higher amounts of acrylic acid increased the amount of carboxylic acid, the mass swelling significantly decreases on both swelling media. This strongly suggests that swelling ability of the hydrogel primarily depends on the crosslinking density increased by the acrylic acid than the deprotonation of its pendent carboxylic acid. Similar findings are also reported elsewhere (63, 108, 109).

3.3.3 Mechanical Properties of PPEGMC

Matching the mechanical properties of the scaffolding material to that of native tissue is one of the governing requirement of tissue engineering. As seen in table 1.2, various soft tissues have their ultimate tensile strength and young's modulus within few hundered kilo pascals. One of the objective of developing PPEGMC is to create polymeric networks with the mechanical properties similar to these soft tissues. The ultimate tensile strength of PPEGMC networks range from 189.14±19.67 to 961.50±60.83 kPa and initial modulus range from 84±18.39 to 1198.57±45.68 kPa. It was observed that for PPEGMCs with higher amounts of cirtic acid, the tensile strength increased and initial modulus decreased (figure 3.7a). For instance, PPEGMC 4/6 displayed a tensile strength of 702.38±62.12 kpa and initial modulus of 388.70±54.83 kpa as compared to PPEGMC8/2 which showed a tensile strength of 304.39±13.43 kpa and initial modulus of 777.20±109.37 kpa. Similarly, increasing the concerntration of crosslinker from 1.5 to 6% results in the formation of PPEGMC networks with 10 fold increase in both tensile strength and initial modulus (figure 3.7b). This may be due to the fact that strong hydrogen bonding among carboxylic acids from cirtic aicd and acrylic acid (crosslinker) have higher impact on the ultimate tensile strength of the networks. Whereas, increase in the crosslinking density due to increase in vinyl functionalities in the polymer networks contributed by maleic acid and acrylic acid have higher influence on the initial modulus of the polymer.

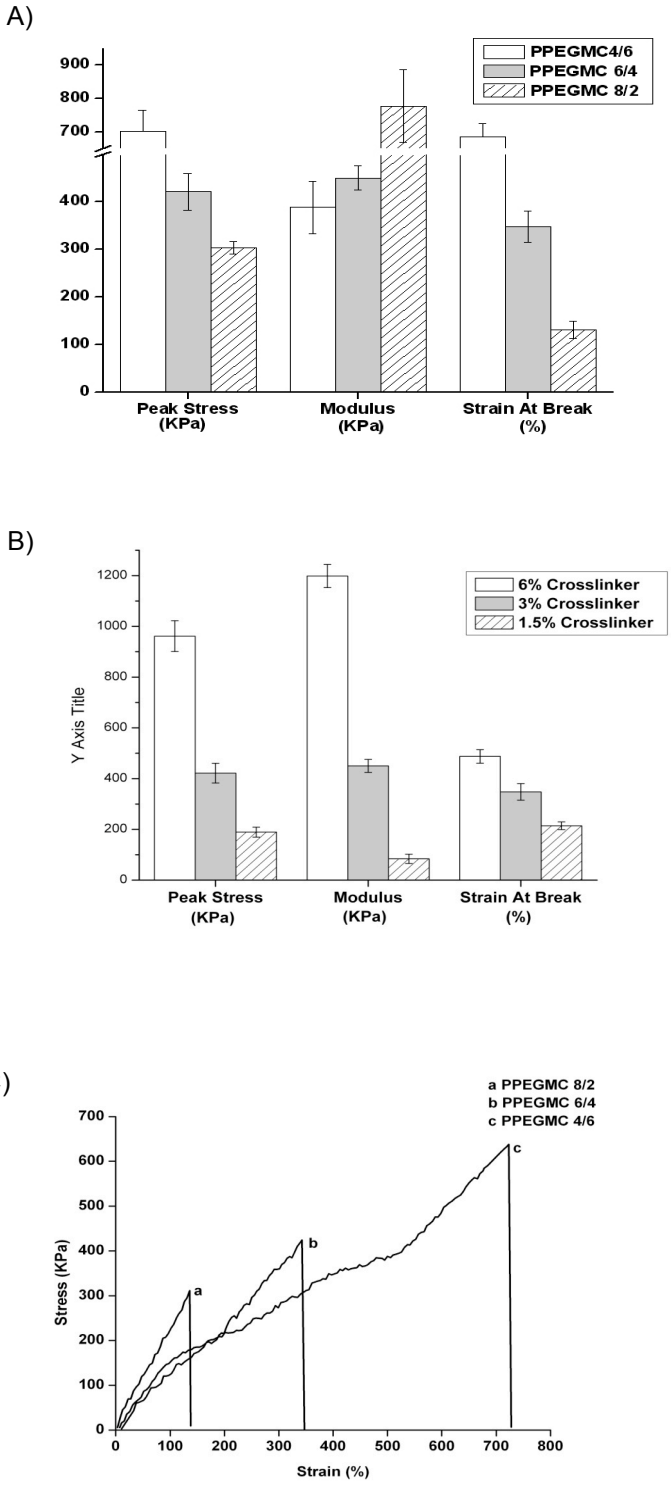

Figure 3.7 Mechanical Properties of PPEGMC hydrogels A) effect of MA/CA ratios, B) effect of crosslinkers, and C) stress vs strain curve of PPEGMCs (n=6).

Another major requirement of material for soft tissue engineering is elastic property and 100% recovery from deformation. This property is absent for most of the FDA approved polymers such as PEG, PLA ,and PGA limiting their uses in soft tissue engineering. As seen in figure 3.7c, the stress-strain curves of various PPEGMC networks showed no yield point, which hints in the ability of the polymer to avoid permanent deformation. Similarly, PPEGMC networks are also highly elastic in nature. For example, the elongation at break of PPEGMC with different ratio of acids ranges from 685.07±40.97 to 131.40±17.78% for PPEGMC4/6 and PPEGMC8/2 respectively (Figure 3.7a). Elongation at break for PPEGMC with different concentration of crosslinker ranges from 487.53±26.86 to 214.03±15.06 for 6% and 1.5% of crosslinker respectively (Figure 3.7b).

3.3.4 In Vitro Degradation Study

In vitro degradation rates of PPEGMC with different molar ratio of acids and different concentration of crosslinker were investigated by examining the change of mass loss for 1 month time period in phosphate buffer solution (pH 7.4 and 37ºC). As shown in figure 3.8a, PPEGMC 8/2 shows the minimal mass loss of 60% where as PPEGMC 4/6 shows complete degradation within 1-month period. Similarly, when PPEGMC 6/4 was crosslinked with different crosslinker concentration, it was observed that 6% of crosslinker shows slower degradation (65% within 1 month) rate than 3% (80% of initial weight) and 1.5% (complete degradation) (Figure 3.8b). These results indicate that amount of vinyl moieties (increased crosslink density) in the polymer precursor has significant effect in the overall degradation profile of the polymer. These results are in agreement with the finding of swelling data, that the hydrogel with highest swelling ability in PBS has fastest degradation rate. Similarly, the morphology of the PPEGMC 6/4 hydrogel crosslinked with 3% of crosslinker was observed at various time periods by SEM (figure 3.8c-e). Surface morphology of freeze-dried hydrogels exhibits highly porous structure and maintained its networking throughout the degradation. This could be beneficial for a cell carrying scaffolds where cell infiltration and tissue formation is the primary objective.

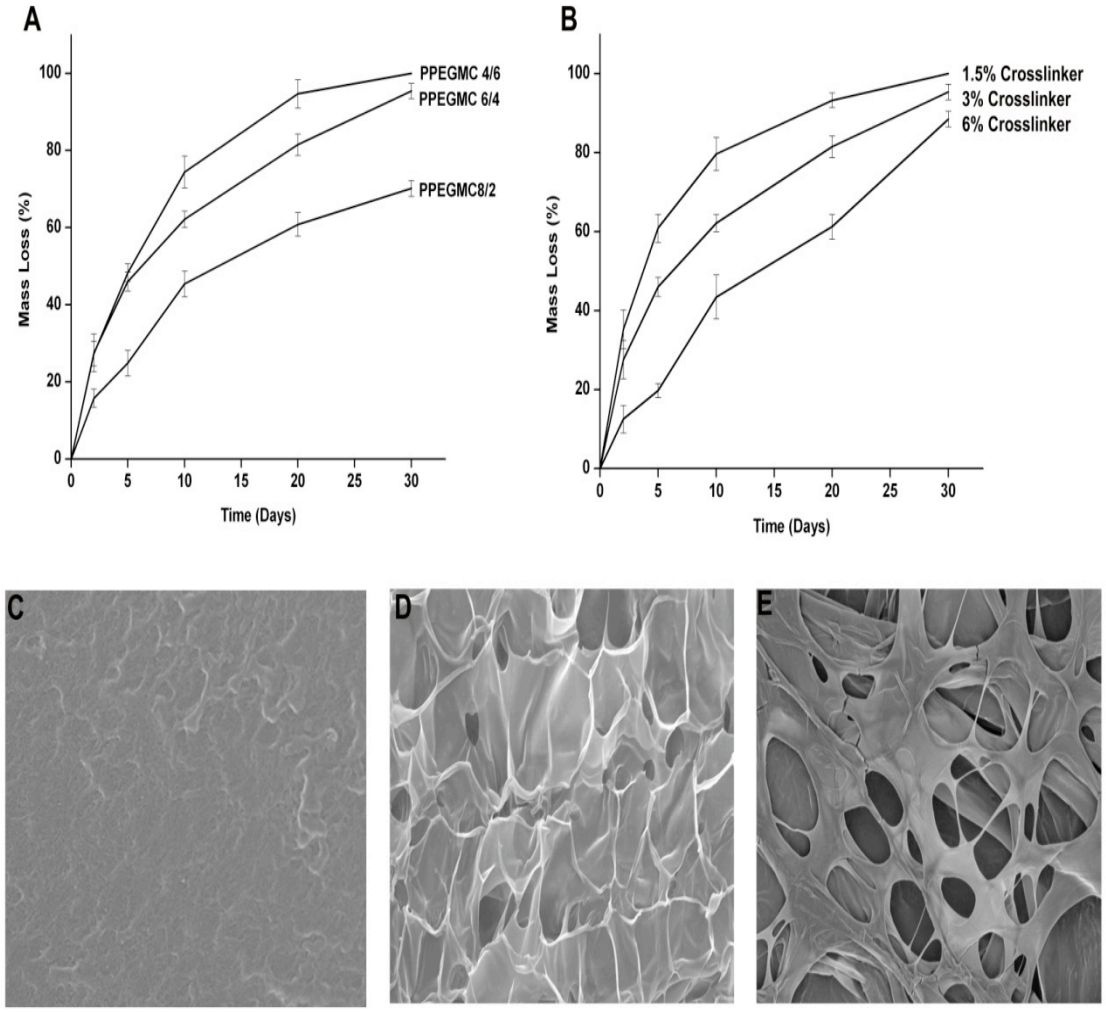

Figure 3.8 The mass loos of the PPEGMC hydrogel during degradation: A) PPEGMC8/2, PPEGMC 6/4, and PPEGMC 4/6 with 3% crosslinker. B) PPEGMC 6/4 with 1.5, 3, and 6% crosslinker (n=6). C) Surface of PPEGMC6/4 at day 1. D) day 7. E) day 20 after incubation in PBS (pH 7.4 and 37ºC).

3.3.5 Drug Release from Hydrogel

As it was observed that the swelling gradient was highest between pH 5.4 and 7.4, so the release profiles of BSA from PPEGMC hydrogels were studied in PBS solution (pH 7.4 and 37 ºC) and in citric acid and potassium dihydrogen phosphate solution (pH 5.4 and 37 ºC). Figure 3.9a-c, shows that at pH 7.4, 92.71±2.01, 85.18±3.83, and 73.08±1.85 % of BSA was

release from PPEGMC 4/6, PPEGMC6/4, and PPEGMC8/2 respectively within a 5 day time period. At pH 7.4, the BSA release percentages were 28.23±1.38, 32.15±3.51, and 61.78±2.87 for respective hydrogels within same period of time. The most remarkable control in the drug release behavior by the pH changes was found in PPEGMC 4/6 and PPEGMC6/4. These results show good agreement with the swelling behavior of PPEGMC at different pH buffers, concluding that a higher amount of carboxylic acid contributed by citric acids in the polymeric chain have the prime control over the releasing profile of the PPEGMC hydrogel. As pH is one of the basic characteristic of body fluid, PPEGMC can act as a “smart” polymeric network for the control release of drugs where pH is the primarily factor of the environment.

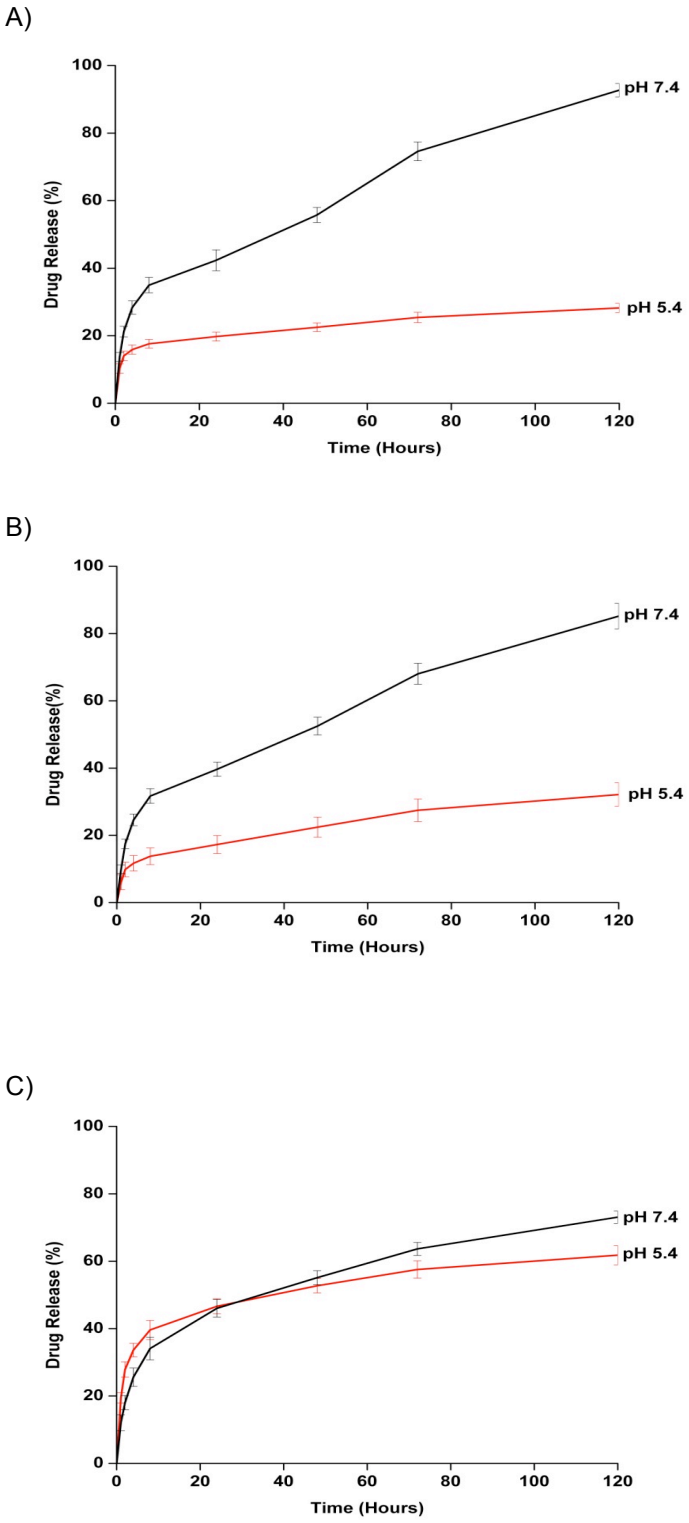

Figure 3.9 Cumulative release of BSA from PPEGMC hydrogels at 37 °C in buffer solution of pH 7.4 and pH 5.4. A) PPEGMC 4/6, B) PPEGMC 6/4, and C) PPEGMC 8/2 (n=7).

3.3.6 PPEGMC Scaffold Fabrication

As mentioned earlier, one of the major requirements of ISCs is their ability to create a porous matrix for the successful in growth of tissue throughout the matrix. For this purpose, gas-forming techniques were utilized in this study. Basically, calcium carbonate was allowed to react with the acidic pendant group of PPEGMC to generate carbon dioxide (CO_2). Bubbles of CO_2 were trapped into the matrix of PPEGMC and quickly crosslinked under photo irradiation. Figure 4.10 shows the surface and cross sectional morphology of the generated scaffold. Average pore sizes of 100-200 μm with some interconnectivity were observed throughout the scaffold.

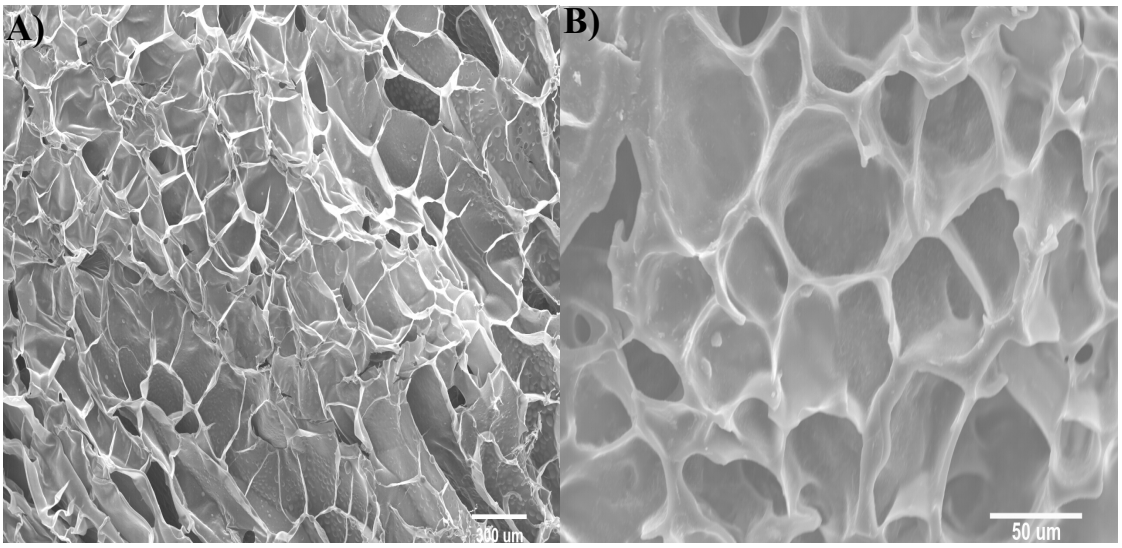

Figure 3.10 SEM micrograph of PPEGMC scaffold fabricated by gas forming technique. A) surface morphology, and B) cross sectional view of the scaffold.

3.3.7 Cytocompatibility of PPEGMC

NIH-3T3 fibroblasts were seeded on PPEGMC hydrogel surfaces. Due to the transpatent nature of the hydrogel, phase-contrast inverted light microscope was used to study the cell morphology in the hydrogels. As seen in figure 3.10, cells were attached and proliferated all over the surface within 3 days period. This demonstrates that PPEGMC hydrogel can be used as a substrate for cell adhesion and proliferation without any pre-treatment or pre-coating of the surface.

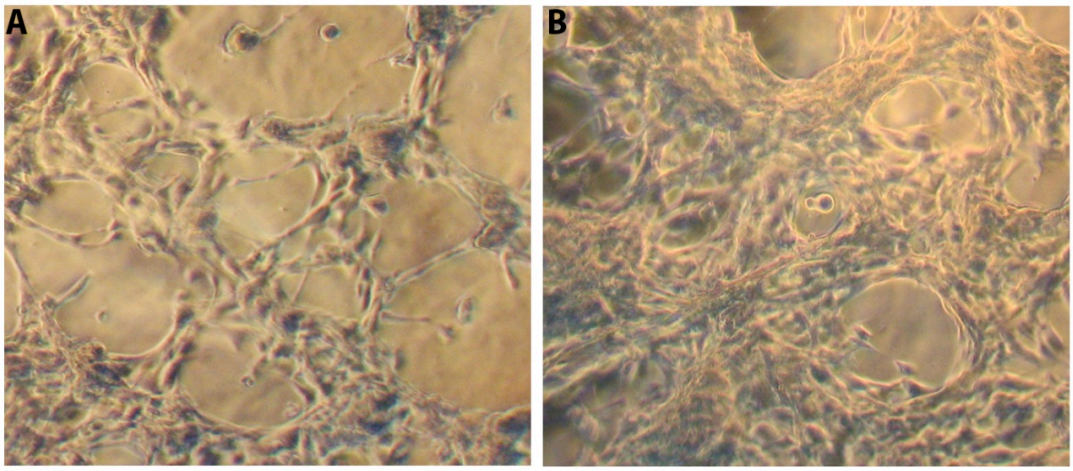

Figure 3.11 Phase contrast Micrographs of NIH-3T3 cell lines cultured on the surface of the hydrogel networks for A) 24h and B) 72h.

NIH-3T3 fibroblasts were also tagged with green fluorescent cell tracer (CFDA-SE) and were encapsulated into the PPEGMC networks. Hydrogels were observed under microscope after 1h of encapsulation and was found that cells were homogeneously distributed throughout the hydrogel (figure 3.11a). After incubation for 24h of the cells encapsulated hydrogels, it was noted that cells were actively elongating and spreading within the networks.

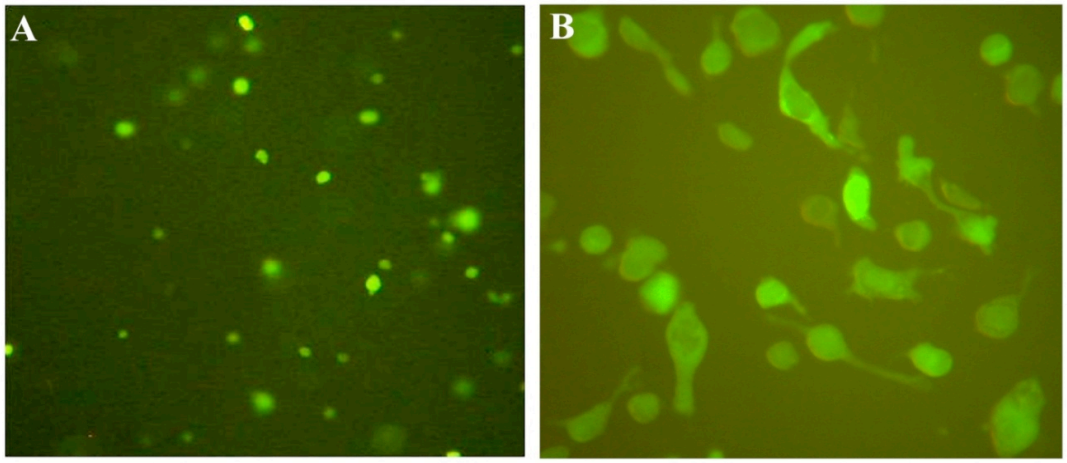

Figure 3.12 Phase contrast micrographs of NIH-3T3 cell lines encapsulate inside the hydrogel networks for A) 1h and B) 24h. Cell lines were tagged with CFDA-SE green fluorescent cell tracer.

3.4 Conclusion

A water soluble, random block pre-polymer was synthesized from PEG200, maleic acid, and citric acid utilizing a controlled polycondensation procedure. These polymeric chains were characterized as a polyester containing vinyl moieties and abundant pendent carboxylic and hydroxyl functionalities. These chains were further polymerized into crosslinked networks by free radical crosslinking mechanism. Physicochemical test demonstrate that these crosslinked networks behave as hydrogel and shows sensitivity in their swelling behavior towards change in pH of the swelling media. Mechanical evaluation of these networks demonstrates that they are highly elastic in their non-hydrated state and possess a close range of mechanical properties to that of native soft tissues. In vitro degradation demonstrates complete degradability of these networks within one month period. These PPEGMCs also shows pH-dependent drug release behavior that correlate with its pH-dependent swelling behavior. Cell encapsulated into the networks and seeded on the surface shows that PPEGMC can be used as a matrix for cell delivery. Thus, PPEGMC should find its uses in numerous tissue engineering and drug delivery applications as an injectable hydrogel.

CHAPTER 4

LIMITATIONS AND FUTURE WORK

In the course of developing an in situ crosslinkable material for tissue engineering and drug delivery application, we have developed two materials, POMC and PPEGMC. The synthesis of the polymers and detailed material characterizations were initial steps to understand the versatile nature of these networks. In vitro degradation and preliminarily biocompatibility tests of these materials show their application in numerous biomedical applications.

4.1 Limitations

All though POMC was synthesized as low molecular weight pre-polymer to serve as injectable material. Its poor solubility in water may limit its ability to tailor its mechanical, swelling, degrading, and biomolecules/cells encapsulating capability. This limitation can be overcome by using its water-soluble counterpart, PPEGMC.

- POMC has high sol content after crosslinking. This may create undesirable leaching of the pre-polymer. This limitation can be overcome by the use of terminal alkene containing crosslinkers.
- Higher amounts of photoinitiator (1 w/w%) were used in this study. This limitation can be overcome by finding a trade-off between crosslinking time, physical, and mechanical properties of the polymer.
- PPEGMC cannot be crosslinked without the use of terminal alkene containing crosslinker. This limitation can be overcome by replacing maleic acid with terminal alkene containing diacid such as itaconic acid.

4.2 Future Work Recommendations

- Biocompatibility of this in situ crosslinkable was performed in vivo with pre-fabricated film. A detail study of POMC/PPEGMC should be performed in vivo with cell/drugs encapsulated as an injectable material.
- Actual gelation time of the pre-polymer should be studied using rheological experiments.
- Physical and mechanical characteristic of the polymer should be performed using redox crosslinking mechanism to understand the performance of these polymers for application where light penetration is limited.
- The wide range of properties of these material show their potential in various application including orthopedics, wound management, and soft tissue engineering. Specific application oriented studies should be done to appreciate the potential of these materials in biomedical applications.

CHAPTER 5

CONCLUSION

The goal of this research work was to develop soft and elastic in situ crosslinkable biomaterials with abundant available attachment sites for bioactive molecules. ISC materials hold great potential for tissue engineering applications by filling irregular defects through a minimally invasive delivery method. ISC materials are also well recognized in the field of drug delivery, as they offer site specific delivery, thus avoiding severe side effects and improving the therapeutic efficacy. The work was initiated with synthesis of a low molecular weight pre-polymer that can be injectable through small diameter syringe. These polymeric networks can be synthesized into water soluble or non-water soluble networks with the choice of monomers according to the need of application. The structural composition of the pre-polymer was characterized using various techniques and confirmed the presence of degradable ester bonds and vinyl moieties on the back bone and pendent carboxylic and hydroxyl functionalities. These pre-polymeric chains were further crosslinked by photocrosslinking and redox crosslinking mechanism to form a novel elastic networks. The chemical, physicochemical, thermal and mechanical properties of the hydrogels were studied with various compositions such as monomers ratio, initiator, crosslinker, and polymer concentrations. These networks demonstrate a close range of ultimate tensile strength and initial modulus as that of various soft tissues. In addition, these networks are highly elastic in nature and show 100% recovery from deformation. In vitro degradation study in PBS illustrates the degradability of the networks. The degradation can be tailored by the choice of diols and molar ratio of citric acid in the backbone of the pre-polymer chain. Due to available pendant functionalities, these networks can easily be

conjugated with bioactive molecules to enhance cellular responses. In vivo biocompatibility evaluation suggested that POMCs are biocompatible materials and degraded products are non-toxic. Ease of processability is another advantage of these ISC polymers. As, the crosslinking can be done by photocrosslinking or redox crosslinking, POMCs enjoys the benefit of both as can be use in numerous application. We have demonstrated the ability of POMCs to fabricate into porous scaffolds, and nanoparticles and hydrogels for drug delivery applications. Interestingly, due to presence of carboxylic acids as pendant group, these networks show pH-dependency in their swelling behavior demonstrating a controlled release of drug at different pH of releasing the media. Thus, POMCs holds great potential as an injectable material with drugs or cell encapsulated into their networks.

REFERENCES

1. Kretlow, J.D., Klouda, L., and Mikos, A.G. Injectable matrices and scaffolds for drug delivery in tissue engineering. Advanced Drug Delivery Reviews 59, 263, 2007.

2. He, D.M., Susanto, H., and Ulbricht, M. Photo-irradiation for preparation, modification and stimulation of polymeric membranes. Progress in Polymer Science 34, 62, 2009.

3. Prestwich, G.D., Shu, X.Z., Liu, Y.C., Cai, S.S., Walsh, J.F., Hughes, C.W., Ahmad, S., Kirker, K.R., Yu, B.L., Orlandi, R.R., Park, A.H., Thibeault, S.L., Duflo, S., and Smith, M.E. Injectable synthetic extracellular matrices for tissue engineering and repair. Tissue Engineering 585, 125, 2006.

4. Anseth, K.S., Metters, A.T., Bryant, S.J., Martens, P.J., Elisseeff, J.H., and Bowman, C.N. In situ forming degradable networks and their application in tissue engineering and drug delivery. Journal of Controlled Release 78, 199, 2002.

5. Rizzi, S.C., Xie, Y., Dawson, R., Ehrbar, M., Hubbell, J.A., Lutolf, M.P., and Upton, Z. Injectable biomimetic matrices to guide impaired wound healing. Wound Repair and Regeneration 16, A62, 2008.

6. Lambert, W.J., and Peck, K.D. Development of an in-Situ Forming Biodegradable Poly-Lactide-Co-Glycolide System for the Controlled-Release of Proteins. Journal of Controlled Release 33, 189, 1995.

7. Temenoff, J.S., Shin, H., Conway, D.E., Engel, P.S., and Mikos, A.G. In vitro cytotoxicity of redox radical initiators for cross-linking of oligo(poly(ethylene glycol) fumarate) macromers. Biomacromolecules 4, 1605, 2003.

8. Orkisz, M.J., Bromberg, L., Pike, R., Lupton, E.C., and Ron, E.S. Rheological properties of reverse thermogelling poly(acrylic acid)-g-(oxyethylene-b-oxypropylene-b-oxyethylene)

polymers (Smart Hydrogel(TM)). Abstracts of Papers of the American Chemical Society 213, 169, 1997.

9. Rowley, J.A., Madlambayan, G., and Mooney, D.J. Alginate hydrogels as synthetic extracellular matrix materials. Biomaterials 20, 45, 1999.

10. Rosler, A., Vandermeulen, G.W.M., and Klok, H.A. Advanced drug delivery devices via self-assembly of amphiphilic block copolymers. Advanced Drug Delivery Reviews 53, 95, 2001.

11. Bakhshi, R., Vasheghani-Farahani, E., Mobedi, H., Jamshidi, A., and Khakpour, M. The effect of additives on naltrexone hydrochloride release and solvent removal rate from an injectable in situ forming PLGA implant. Polymers for Advanced Technologies 17, 354, 2006.

12. Davis, K.A., Burdick, J.A., and Anseth, K.S. Photoinitiated crosslinked degradable copolymer networks for tissue engineering applications. Biomaterials 24, 2485, 2003.

13. Timmer, M.D., Ambrose, C.G., and Mikos, A.G. Evaluation of thermal- and photo-crosslinked biodegradable poly(propylene fumarate)-based networks. Journal of Biomedical Materials Research Part A 66A, 811, 2003.

14. Holland, T.A., Bodde, E.W.H., Baggett, L.S., Tabata, Y., Mikos, A.G., and Jansen, J.A. Osteochondral repair in the rabbit model utilizing bilayered, degradable oligo(poly(ethylene glycol) fumarate) hydrogel scaffolds. Journal of Biomedical Materials Research Part A 75A, 156, 2005.

15. Xia, X.H., Hu, Z.B., and Marquez, M. Physically bonded nanoparticle networks: a novel drug delivery system. Journal of Controlled Release 103, 21, 2005.

16. Zhu, W., and Ding, J.D. Synthesis and characterization of a redox-initiated, injectable, biodegradable hydrogel. Journal of Applied Polymer Science 99, 2375, 2006.

17. Yan, D.Y., and Wang, W.X. "Living"/controlled radical polymerization initiated by redox system. Abstracts of Papers of the American Chemical Society 218, U490, 1999.

18. Atici, O.G., Akar, A., Ayar, Y., and Mecit, O. Synthesis of block copolymers via redox polymerization. Journal of Applied Polymer Science 71, 1385, 1999.

19. Shu, X.Z., Liu, Y.C., Palumbo, F.S., Lu, Y., and Prestwich, G.D. In situ crosslinkable hyaluronan hydrogels for tissue engineering. Biomaterials 25, 1339, 2004.

20. Hillwest, J.L., Chowdhury, S.M., Slepian, M.J., and Hubbell, J.A. Inhibition of Thrombosis and Intimal Thickening by in-Situ Photopolymerization of Thin Hydrogel Barriers. Proceedings of the National Academy of Sciences of the United States of America 91, 5967, 1994.

21. Nguyen, K.T., and West, J.L. Photopolymerizable hydrogels for tissue engineering applications. Biomaterials 23, 4307, 2002.

22. Burdick, J.A., Peterson, A.J., and Anseth, K.S. Conversion and temperature profiles during the photoinitiated polymerization of thick orthopaedic biomaterials. Biomaterials 22, 1779, 2001.

23. Ifkovits, J.L., and Burdick, J.A. Review: Photopolymerizable and degradable biomaterials for tissue engineering applications. Tissue Engineering 13, 2369, 2007.

24. Decker, C. Uv-Curing Chemistry - Past, Present, and Future. Journal of Coatings Technology 59, 97, 1987.

25. Fisher, J.P., Dean, D., Engel, P.S., and Mikos, A.G. Photoinitiated polymerization of biomaterials. Annual Review of Materials Research 31, 171, 2001.

26. Bryant, S.J., Nuttelman, C.R., and Anseth, K.S. Cytocompatibility of UV and visible light photoinitiating systems on cultured NIH/3T3 fibroblasts in vitro. Journal of Biomaterials Science-Polymer Edition 11, 439, 2000.

27. Nerem, R.M. Tissue engineering: The hope, the hype, and the future. Tissue Engineering 12, 1143, 2006.

28. Lavik, E., and Langer, R. Tissue engineering: current state and perspectives. Applied Microbiology and Biotechnology 65, 1, 2004.

29. Langer, R., and Vacanti, J.P. Tissue Engineering. Science 260, 920, 1993.

30. Drury, J.L., and Mooney, D.J. Hydrogels for tissue engineering: scaffold design variables and applications. Biomaterials 24, 4337, 2003.

31. Deb, S., Braden, M., and Bonfield, W. Effect of crosslinking agents on poly(ethylmethacrylate) bone cements. Journal of Materials Science-Materials in Medicine 8, 829, 1997.

32. Hoffmann, B., Volkmer, E., Kokott, A., Weber, M., Hamisch, S., Schieker, M., Mutschler, W., and Ziegler, G. A new biodegradable bone wax substitute with the potential to be used as a bone filling material. Journal of Materials Chemistry 17, 4028, 2007.

33. Hou, Q.P., De Bank, P.A., and Shakesheff, K.M. Injectable scaffolds for tissue regeneration. Journal of Materials Chemistry 14, 1915, 2004.

34. Tate, M.C., Shear, D.A., Hoffman, S.W., Stein, D.G., and LaPlaca, M.C. Biocompatibility of methylcellulose-based constructs designed for intracerebral gelation following experimental traumatic brain injury. Biomaterials 22, 1113, 2001.

35. Suggs, L.J., Shive, M.S., Garcia, C.A., Anderson, J.M., and Mikos, A.G. In vitro cytotoxicity and in vivo biocompatibility of poly(propylene fumarate-co-ethylene glycol) hydrogels. Journal of Biomedical Materials Research 46, 22, 1999.

36. Amsden, B.G., Misra, G., Gu, F., and Younes, H.M. Synthesis and characterization of a photo-cross-linked biodegradable elastomer. Biomacromolecules 5, 2479, 2000.

37. Bettinger, C.J., Bruggeman, J.P., Borenstein, J.T., and Langer, R.S. Amino alcohol-based degradable poly(ester amide) elastomers. Biomaterials 29, 2315, 2008.

38. Wang, Y.D., Ameer, G.A., Sheppard, B.J., and Langer, R. A tough biodegradable elastomer. Nature Biotechnology 20, 602, 2002.

39. Ding, T., Liu, Q.Y., Shi, R., Tian, M., Yang, H., and Zhang, L.Q. Synthesis, characterization and in vitro degradation study of a novel and rapidly degradable elastomer. Polymer Degradation and Stability 91, 733, 2006.

40. Wan, Y.Q., Feng, G., Shen, F.H., Balian, G., Laurencin, C.T., and Li, X.D. Novel biodegradable poly(1,8-octanediol malate) for annulus fibrosus regeneration. Macromolecular Bioscience 7, 1217, 2007.

41. Yang, J., Webb, A.R., Pickerill, S.J., Hageman, G., and Ameer, G.A. Synthesis and evaluation of poly(diol citrate) biodegradable elastomers. Biomaterials 27, 1889, 2006.

42. Dahms, S.E., Piechota, H.J., Dahiya, R., Lue, T.F., and Tanagho, E.A. Composition and biomechanical properties of the bladder acellular matrix graft: comparative analysis in rat, pig and human. British Journal of Urology 82, 411, 1998.

43. Nakano, K., Sugawara, M., Ishihara, K., Kanazawa, S., Corin, W.J., Denslow, S., Biederman, R.W.W., and Carabello, B.A. Myocardial Stiffness Derived from End-Systolic Wall Stress and Logarithm of Reciprocal of Wall Thickness - Contractility Index Independent of Ventricular Size. Circulation 82, 1352, 1990.

44. Sung, H.W., Chang, Y., Chiu, C.T., Chen, C.N., and Liang, H.C. Mechanical properties of a porcine aortic valve fixed with a naturally occurring crosslinking agent. Biomaterials 20, 1759, 1999.

45. Webb, A.R., Yang, J., and Ameer, G.A. Biodegradable polyester elastomers in tissue engineering. Expert Opinion on Biological Therapy 4, 801, 2004.

46. Gupta, B.S., and Kasyanov, V.A. Biomechanics of human common carotid artery and design of novel hybrid textile compliant vascular grafts. Journal of Biomedical Materials Research 34, 341, 1997.

47. Shepherd, D.E.T., Seedhom, B.B., and Mann, R.W. A technique for measuring the compressive modulus of articular cartilage under physiological loading rates with preliminary results. Proceedings of the Institution of Mechanical Engineers Part H-Journal of Engineering in Medicine 213, 291, 1999.

48. Gunatillake, P.A., and Adhikari, R. Biodegradable synthetic polymers for tissue engineering. Eur Cell Mater 5, 1, 2003.

49. Okada, M. Chemical syntheses of biodegradable polymers. Progress in Polymer Science 27, 87, 2002.

50. Tokiwa, Y., and Calabia, B.P. Biodegradability and biodegradation of poly(lactide). Applied Microbiology and Biotechnology 72, 244, 2006.

51. Steffens, G.C.M., Nothdurft, L., Buse, G., Thissen, H., Hocker, H., and Klee, D. High density binding of proteins and peptides to poly(D,L-lactide) grafted with polyacrylic acid. Biomaterials 23, 3523, 2002.

52. Lutz, J.F., and Borner, H.G. Modern trends in polymer bioconjugates design. Progress in Polymer Science 33, 1, 2008.

53. Veronese, F.M., and Morpurgo, M. Bioconjugation in pharmaceutical chemistry. Farmaco 54, 497, 1999.

54. Cook, A.D., Hrkach, J.S., Gao, N.N., Johnson, I.M., Pajvani, U.B., Cannizzaro, S.M., and Langer, R. Characterization and development of RGD-peptide-modified poly(lactic acid-co-lysine) as an interactive, resorbable biomaterial. Journal of biomedical materials research 35, 513, 1997.

55. Nam, Y.S., Yoon, J.J., Lee, J.G., and Park, T.G. Adhesion behaviours of hepatocytes cultured onto biodegradable polymer surface modified by alkali hydrolysis process. Journal of biomaterials science 10, 1145, 1999.

56. Yong Zhang, W.W., Qingling Feng, Fuzhai Cui , Yingxin Xu. A novel method to immobilize collagen on polypropylene film as substrate for hepatocyte culture. Materials Science and Engineering C 26, 657 2006.

57. Nitschke, M., Schmack, G., Janke, A., Simon, F., Pleul, D., and Werner, C. Low pressure plasma treatment of poly(3-hydroxybutyrate): toward tailored polymer surfaces for tissue engineering scaffolds. Journal of biomedical materials research 59, 632, 2002.

58. Breunig, M., Bauer, S., and Goefferich, A. Polymers and nanoparticles: Intelligent tools for intracellular targeting? European Journal of Pharmaceutics and Biopharmaceutics 68, 112, 2008.

59. Wei, G.B., Jin, Q.M., Giannobile, W.V., and Ma, P.X. Nano-fibrous scaffold for controlled delivery of recombinant human PDGF-BB. Journal of Controlled Release 112, 103, 2006.

60. Patri, A.K., Kukowska-Latallo, J.F., and Baker, J.R., Jr. Targeted drug delivery with dendrimers: comparison of the release kinetics of covalently conjugated drug and non-covalent drug inclusion complex. Adv Drug Deliv Rev 57, 2203, 2005.

61. Langer, R. Drug delivery and targeting. Nature 392, 5, 1998.

62. Sahiner, N., Godbey, W.T., McPherson, G.L., and John, V.T. Microgel, nanogel and hydrogel-hydrogel semi-IPN composites for biomedical applications: synthesis and characterization. Colloid and Polymer Science 284, 1121, 2006.

63. Wu, D.Q., Sun, Y.X., Xu, X.D., Cheng, S.X., Zhang, X.Z., and Zhuo, R.X. Biodegradable and pH-sensitive hydrogels for cell encapsulation and controlled drug release. Biomacromolecules 9, 1155, 2008.

64. Hatefi, A., and Amsden, B. Biodegradable injectable in situ forming drug delivery systems. Journal of Controlled Release 80, 9, 2002.

65. Karp, J.M., and Langer, R. Development and therapeutic applications of advanced biomaterials. Current Opinion in Biotechnology 18, 454, 2007.

66. Adams, M.L., Lavasanifar, A., and Kwon, G.S. Amphiphilic block copolymers for drug delivery. Journal of Pharmaceutical Sciences 92, 1343, 2003.

67. Torchilin, V.P., and Trubetskoy, V.S. Which Polymers Can Make Nanoparticulate Drug Carriers Long-Circulating. Advanced Drug Delivery Reviews 16, 141, 1995.

68. Whiteman, K.R., Subr, V., Ulbrich, K., and Torchilin, V.P. Poly(HPMA)-coated liposomes demonstrate prolonged circulation in mice. Journal of Liposome Research 11, 153, 2001.

69. Lei, L.J., Ding, T., Shi, R., Liu, Q.Y., Zhang, L.Q., Chen, D.F., and Tian, W. Synthesis, characterization and in vitro degradation of a novel degradable poly((1,2-propanediol-sebacate)-citrate) bioelastomer. Polymer Degradation and Stability 92, 389, 2007.

70. Dey, J., Xu, H., Shen, J.H., Thevenot, P., Gondi, S.R., Nguyen, K.T., Sumerlin, B.S., Tang, L.P., and Yang, J. Development of biodegradable crosslinked urethane-doped polyester elastomers. Biomaterials 29, 4637, 2008.

71. Kang, Y., Yang, J., Khan, S., Anissian, L., and Ameer, G.A. A new biodegradable polyester elastomer for cartilage tissue engineering. Journal of Biomedical Materials Research Part A 77A, 331, 2006.

72. Chen, Q.Z., Bismarck, A., Hansen, U., Junaid, S., Tran, M.Q., Harding, S.E., Ali, N.N., and Boccaccini, A.R. Characterisation of a soft elastomer poly(glycerol sebacate) designed to match the mechanical properties of myocardial tissue. Biomaterials 29, 47, 2008.

73. Yang, J., Webb, A.R., and Ameer, G.A. Novel citric acid-based biodegradable elastomers for tissue engineering. Advanced Materials 16, 511, 2004.

74. Nijst, C.L.E., Bruggeman, J.P., Karp, J.M., Ferreira, L., Zumbuehl, A., Bettinger, C.J., and Langer, R. Synthesis and characterization of photocurable elastomers from poly(glycerol-co-sebacate). Biomacromolecules 8, 3067, 2007.

75. Gerecht, S., Townsend, S.A., Pressler, H., Zhu, H., Nijst, C.L.E., Bruggeman, J.P., Nichol, J.W., and Langer, R. A porous photocurable elastomer for cell encapsulation and culture. Biomaterials 28, 4826, 2007.

76. Peppas, N.A., Keys, K.B., Torres-Lugo, M., and Lowman, A.M. Poly(ethylene glycol)-containing hydrogels in drug delivery. Journal of Controlled Release 62, 81, 1999.

77. Langer, R., and Peppas, N.A. Advances in biomaterials, drug delivery, and bionanotechnology. Aiche Journal 49, 2990, 2003.

78. Shu, X.Z., Ahmad, S., Liu, Y.C., and Prestwich, G.D. Synthesis and evaluation of injectable, in situ crosslinkable synthetic extracellular matrices for tissue engineering. Journal of Biomedical Materials Research Part A 79A, 902, 2006.

79. Prestwich, G.D. In situ crosslinkable synthetic extracellular matrices for tissue engineering and repair. Faseb Journal 20, A21, 2006.

80. Nuttelman, C.R., Henry, S.M., and Anseth, K.S. Synthesis and characterization of photocrosslinkable, degradable poly(vinyl alcohol)-based tissue engineering scaffolds. Biomaterials 23, 3617, 2002.

81. Schmedlen, K.H., Masters, K.S., and West, J.L. Photocrosslinkable polyvinyl alcohol hydrogels that can be modified with cell adhesion peptides for use in tissue engineering. Biomaterials 23, 4325, 2002.

82. Fisher, J.P., Tirnmer, M.D., Holland, T.A., Dean, D., Engel, P.S., and Mikos, A.G. Photoinitiated cross-linking of the biodegradable polyester poly(propylene fumarate). Part I. Determination of network structure. Biomacromolecules 4, 1327, 2003.

83. Jo, S., Shin, H., and Mikos, A.G. Modification of oligo(poly(ethylene glycol) fumarate) macromer with a GRGD peptide for the preparation of functionalized polymer networks. Biomacromolecules 2, 255, 2001.

84. Wang, D.A., Williams, C.G., Li, Q.A., Sharma, B., and Elisseeff, J.H. Synthesis and characterization of a novel degradable phosphate-containing hydrogel. Biomaterials 24, 3969, 2003.

85. Li, Q., Wang, J., Shahani, S., Sun, D.D.N., Sharma, B., Elisseeff, J.H., and Leong, K.W. Biodegradable and photocrosslinkable polyphosphoester hydrogel. Biomaterials 27, 1027, 2006.

86. Mizutani, M., and Matsuda, T. Photocurable liquid biodegradable copolymers: In vitro hydrolytic degradation behaviors of photocured films of coumarin-endcapped poly(epsilon-caprolactone-co-trimethylene carbonate). Biomacromolecules 3, 249, 2002.

87. Burdick, J.A., Padera, R.F., Huang, J.V., and Anseth, K.S. An investigation of the cytotoxicity and histocompatibility of in situ forming lactic acid based orthopedic biomaterials. Journal of Biomedical Materials Research 63, 484, 2002.

88. Amoa, K. Catalytic Hydrogenation of Maleic Acid at Moderate Pressures: A Laboratory Demonstration Journal of Chemical Education 84, 1948, 2007.

89. Daruwalla, J., Greish, K., Malcontenti-Wilson, C., Muralidharan, V., Iyer, A., Maeda, H., and Christophi, C. Styrene Maleic Acid-Pirarubicin Disrupts Tumor Microcirculation and Enhances the Permeability of Colorectal Liver Metastases. J Vasc Res 46, 218, 2008.

90. Lu, Y., and Mosier, N.S. Kinetic modeling analysis of maleic acid-catalyzed hemicellulose hydrolysis in corn stover. Biotechnol Bioeng 101, 1170, 2008.

91. Wong, T.W., Wahab, S., and Anthony, Y. Drug release responses of zinc ion crosslinked poly(methyl vinyl ether-co-maleic acid) matrix towards microwave. Int J Pharm 357, 154, 2008.

92. Yang, J., Webb, AR, Hageman, G, Ameer, GA. Novel Citric Acid-Based Biodegradable Elastomers for Tissue Engineering. Advance Materials 16, 511, 2004.

93. Webb, A.R., Yang, J., and Ameer, G.A. Biodegradable polyester elastomers in tissue engineering. Expert Opin Biol Ther 4, 801, 2004.

94. Kang, Y., Yang, J., Khan, S., Anissian, L., and Ameer, G.A. A new biodegradable polyester elastomer for cartilage tissue engineering. J Biomed Mater Res A 77, 331, 2006.

95. Younes, H.M., Bravo-Grimaldo, E., and Amsden, B.G. Synthesis, characterization and in vitro degradation of a biodegradable elastomer. Biomaterials 25, 5261, 2004.

96. Wang, Y., Ameer, G.A., Sheppard, B.J., and Langer, R. A tough biodegradable elastomer. Nat Biotechnol 20, 602, 2002.

97. Yang, J., Webb, A.R., Pickerill, S.J., Hageman, G., and Ameer, G.A. Synthesis and evaluation of poly(diol citrate) biodegradable elastomers. Biomaterials 27, 1889, 2006.

98. Pedersen, L., and Jemec, G.B. Mechanical properties and barrier function of healthy human skin. Acta Derm Venereol 86, 308, 2006.

99. Ma, P.X. Biomimetic materials for tissue engineering. Advanced Drug Delivery Reviews 60, 184, 2008.

100. Yang, J., Bei, J., and Wang, S. Enhanced cell affinity of poly (D,L-lactide) by combining plasma treatment with collagen anchorage. Biomaterials 23, 2607, 2002.

101. Fujita, M., Lee, B.S., Khazenzon, N.M., Penichet, M.L., Wawrowsky, K.A., Patil, R., Ding, H., Holler, E., Black, K.L., and Ljubimova, J.Y. Brain tumor tandem targeting using a combination of monoclonal antibodies attached to biopoly(beta-L-malic acid). J Control Release 122, 356, 2007.

102. Duncanson, W.J., Figa, M.A., Hallock, K., Zalipsky, S., Hamilton, J.A., and Wong, J.Y. Targeted binding of PLA microparticles with lipid-PEG-tethered ligands. Biomaterials 28, 4991, 2007.

103. Hsu, S.H., Whu, S.W., Hsieh, S.C., Tsai, C.L., Chen, D.C., and Tan, T.S. Evaluation of chitosan-alginate-hyaluronate complexes modified by an RGD-containing protein as tissue-engineering scaffolds for cartilage regeneration. Artif Organs 28, 693, 2004.

104. Sakiyama-Elbert, S.E., and Hubbell, J.A. Functional biomaterials: Design of novel biomaterials. Annual Review of Materials Research 31, 183, 2001.

105. Choucair, M., and Phillips, T. A review of wound healing and dressing materials. Wounds-a Compendium of Clinical Research and Practice 8, 165, 1996.

106. Boyce, S.T. Design principles for composition and performance of cultured skin substitutes. Burns 27, 523, 2001.

107. Shi, P.H., Li, Y.G., and Pan, C.Y. Block and star block copolymers by mechanism transformation - X. Synthesis of poly(ethylene oxide) methyl ether/polystyrene/poly(L-lactide) ABC miktoarm star copolymers of by combination of RAFT and ROP. European Polymer Journal 40, 1283, 2004.

108. Zhang, X.Z., Wu, D.Q., and Chu, C.C. Synthesis, characterization and controlled drug release of thermosensitive IPN-PNIPAAm hydrogels. Biomaterials 25, 3793, 2004.

109. Alvarez-Lorenzo, C., and Concheiro, A. Reversible adsorption by a pH- and temperature-sensitive acrylic hydrogel. Journal of Controlled Release 80, 247, 2002.

BIOGRAPHICAL INFORMATION

Dipendra Raj Gyawali was born in Nepal in June of 1982. He came to the United States in 2002 to obtain a Bachelor of Science Degree in Biology. He joined the University of Texas at Arlington as a biology student in January of 2004 but was immediately attracted to the Biomedical Engineering at joint program of University of Texas at Arlington and University of Texas Southwestern Medical Center. His job as a supplemental instructor of Organic Chemistry paved the way for him to join the Biomaterials and Tissue Engineering Research Laboratory at UTA to work under Dr. Jian Yang. His exposure to the latest in biomaterial field during his study led him to believe that biomaterials could be the strongest lead in today's medical studies. Upon completion of his Master of Science degree in May 2009, he intends to continue his research as a Ph.D. candidate. He is a student member of the Biomaterial Society.